



Review

# Meso-Formyl, Vinyl, and Ethynyl Porphyrins—Multipotent Synthons for Obtaining a Diverse Array of Functional Derivatives

Vladimir S. Tyurin <sup>1,\*</sup> , Alena O. Shkirdova <sup>1</sup>, Oscar I. Koifman <sup>2</sup>  and Ilya A. Zamilatskov <sup>1,\*</sup>

<sup>1</sup> Frumkin Institute of Physical Chemistry and Electrochemistry, Russian Academy of Sciences, 119071 Moscow, Russia

<sup>2</sup> Department of Chemistry and Technology of Macromolecular Compounds, Ivanovo State University of Chemistry and Technology, 153000 Ivanovo, Russia; koifman@isuct.ru

\* Correspondence: tv@org.chem.msu.ru (V.S.T.); joz@mail.ru (I.A.Z.)

**Abstract:** This review presents a strategy for obtaining various functional derivatives of tetrapyrrole compounds based on transformations of unsaturated carbon-oxygen and carbon-carbon bonds of the substituents at the *meso* position (*meso*-formyl, vinyl, and ethynyl porphyrins). First, synthetic approaches to the preparation of these precursors are described. Then diverse pathways for the transformations of the multipotent synthons are discussed, revealing a variety of products of such reactions. The structures, electronic, and optical properties of the compounds obtained by the methods under consideration are analyzed. In addition, there is an overview of the applications of the products obtained. Biomedical use of the compounds is among the most important. Finally, the advantages of using the reviewed synthetic strategy to obtain dyes with targeted properties are highlighted.

**Keywords:** *meso*-functionalized porphyrin; *meso*-formylporphyrin; *meso*-vinylporphyrin; *meso*-ethynylporphyrin; porphyrin synthon; Vilsmeier–Haack formylation; Wittig reaction; Schiff base; Heck reaction; Sonogashira reaction; Glaser coupling



**Citation:** Tyurin, V.S.; Shkirdova, A.O.; Koifman, O.I.; Zamilatskov, I.A. *Meso*-Formyl, Vinyl, and Ethynyl Porphyrins—Multipotent Synthons for Obtaining a Diverse Array of Functional Derivatives. *Molecules* **2023**, *28*, 5782. <https://doi.org/10.3390/molecules28155782>

Academic Editor: Alessandro D'Urso

Received: 9 July 2023

Revised: 23 July 2023

Accepted: 25 July 2023

Published: 31 July 2023



**Copyright:** © 2023 by the authors. Licensee MDPI, Basel, Switzerland. This article is an open access article distributed under the terms and conditions of the Creative Commons Attribution (CC BY) license (<https://creativecommons.org/licenses/by/4.0/>).

## 1. Introduction

The production of porphyrin materials with target-specific structures is based on various methodologies, differing in that natural or synthetic porphyrins are used. Naturally derived porphyrins are substituted at  $\beta$ -pyrrolic position and usually with free-from substitution *meso*-carbons. The synthetic porphyrin core can be easily obtained by tetrapyrrole condensation, and the most popular way is condensation of easily available unsubstituted pyrrole with aldehydes to give *meso*-substituted porphyrins [1]. Thus, two main alternative porphyrin types are used as starting materials in synthesis: (1)  $\beta$ -substituted-*meso*-unsubstituted; and (2)  $\beta$ -unsubstituted-*meso*-substituted (Figure 1). Most of the synthetically obtained porphyrins are *meso*-arylporphyrins, like *meso*-tetraphenylporphyrin (TPP) and *meso*-diphenylporphyrin (DPP). The most popular synthetic porphyrin resembling natural porphyrins is  $\beta$ -octaethylporphyrin (OEP). The starting basic tetrapyrroles then need to be functionalized to impart the required properties to the porphyrin molecule [2–4]. The tetrapyrrolic macrocycle can be functionalized by a variety of methods, among which formylation is especially prolific due to the well-developed, very efficient, and easy-to-use formylation methods [5]. The advantage of this functionalization methodology is based on the fact that the aldehyde group is rich in the possibilities of further transformations leading to the addition of functional fragments. The vinyl group is also useful for further functionalizations, and it can be obtained by the Wittig reaction of the formyl-substituted substrate. The acetylenyl group is among the most commonly used for making multichromophore molecules due to its rich coupling possibilities. Thus, formyl, vinyl, and ethynyl groups are magic functions that lead to a variety of products from further transformations, including conversions between them (formyl  $\rightleftharpoons$  ethenyl  $\rightleftharpoons$  ethynyl). The products obtained

through the transformations of these three main synthons are used in a wide variety of applications, including optical sensors [6] and photosensitizers [7–9]. The role of  $\beta$ -formyl and  $\beta$ -vinyl-porphyrins in the synthesis of various porphyrin derivatives was summarized in the review [10]. The  $\beta$ -position is more easily accessible to reagents compared to the *meso* position, and there were a wide variety of products synthesized from  $\beta$ -formyl and  $\beta$ -vinyl-porphyrins. The *meso* position is sterically hindered by the neighboring  $\beta$ -carbon atoms and their substituents, so the reactions of *meso* groups proceed harder. This obstacle is responsible for fewer reported works dealing with *meso* versus  $\beta$  functionalizations and transformations. However, the *meso*-substitution affects the electronic system and spectral properties of the tetrapyrrole macrocycle more strongly. Particularly, the *meso* push-pull substituted porphyrins are the most efficient organic photosensitizers for dye-sensitized solar cells (DSSC) [11]. Thus, it is important to develop *meso* functionalization and transformation methodologies, and the formyl, vinyl, and ethynyl groups present excellent opportunities for primary functionalization and further transformations at the *meso* position.

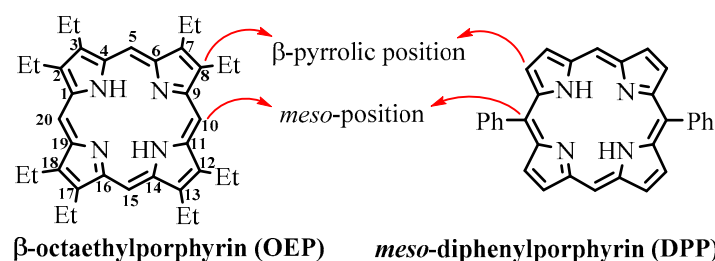


**Figure 1.** Structures of the main porphyrin types: *meso*- and  $\beta$ -substituted, and the numbering of the tetrapyrrolic macrocycle.

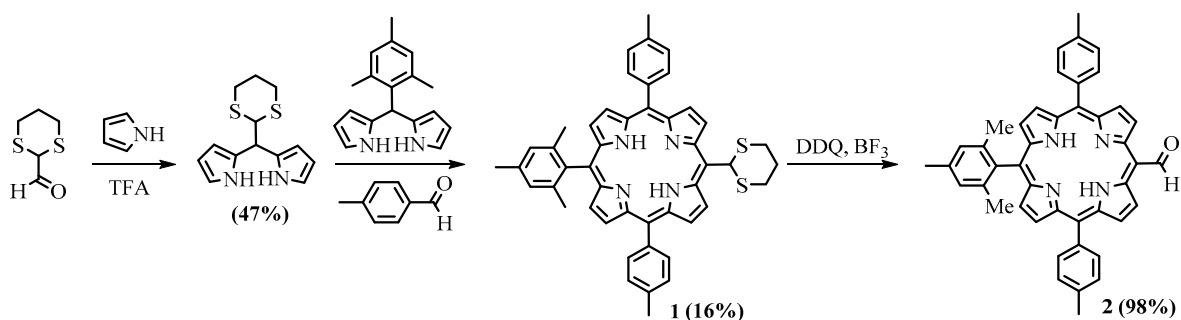
## 2. *Meso*-Formylporphyrins

Insertion of the formyl group into porphyrins is a primary functionalization of the tetrapyrrole ring, opening opportunities for further transformations including, but not limited to, Wittig [12–14], Grignard [14–16], McMurry [17], cycloaddition [18], Knoevenagel [19] reactions, and Schiff bases preparation [20]. Ponomarev made a considerable contribution to the chemistry of formylporphyrins and published a corresponding review about 30 years ago, summarizing works reported up to that date [5].

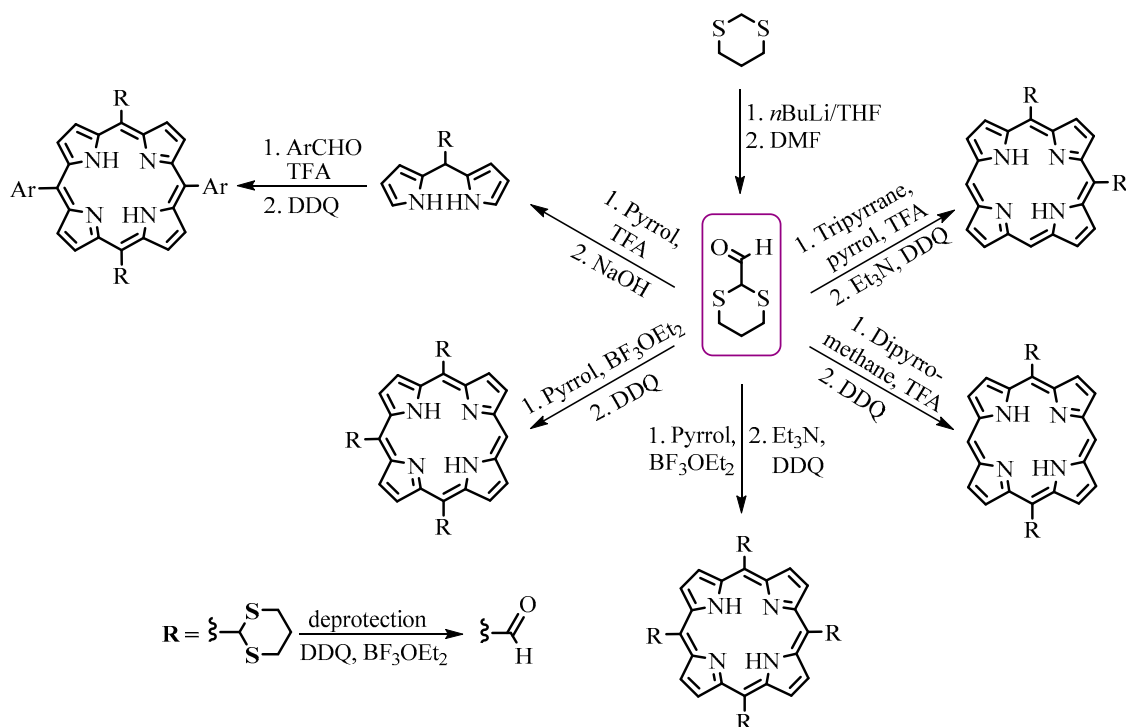
### 2.1. Preparation of *Meso*-Formylporphyrins

One of the strategies for the preparation of functionalized porphyrins is the utilization of the correspondingly functionalized precursors in the synthesis of the porphyrin core. The formyl group is actively involved in the condensation reaction during tetrapyrrole ring construction, and it needs to be protected. Formylporphyrins were obtained by the usual macrocyclization route to the porphyrins from the masked formyl-containing precursors: 2-formyl-1,3-dithiolane was converted to 5-(1,3-dithian-2-yl)dipyrromethane and mixed MacDonald [2 + 2] condensation with 5-mesytyldipyrromethane and *p*-tolualdehyde led to 5-(1,3-dithian-2-yl)-15-mesytyl-10,20-di(4-tolyl)porphyrin **1** which gave the corresponding 5-formyl-15-mesytyl-10,20-di(4-tolyl)porphyrin **2** after deprotection with DDQ/BF<sub>3</sub>(OEt<sub>2</sub>) (Scheme 1) [21].

Similar methods of preparation of formylporphyrins from 1,3-dithiane were proposed by Lindsey [22] and Senge [23]. These methods open opportunities for obtaining 5-, 5,10-, 5,15-, 5,10,15,20-thianyl substituted porphyrins (Scheme 2), which can easily be deprotected to the corresponding formylporphyrins with quantitative yield.

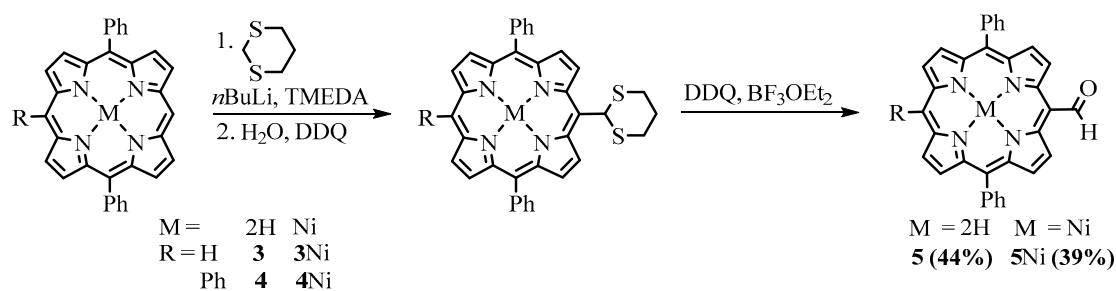


**Scheme 1.** Synthesis of *meso*-formylporphyrin from the semi-protected oxalic aldehyde.



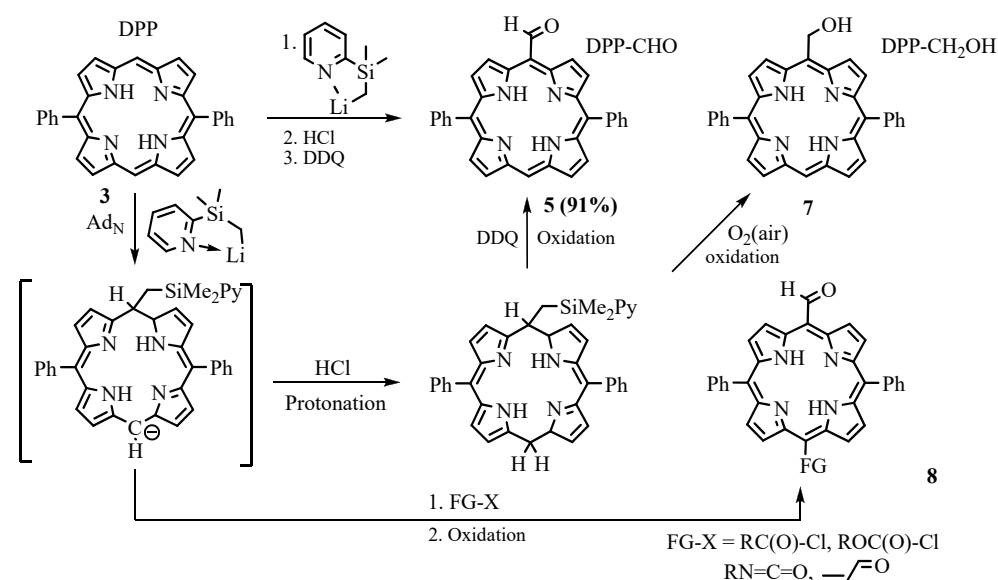
**Scheme 2.** Synthesis of variously substituted *meso*-formylporphyrins.

The insertion of the formyl group into the already assembled tetrapyrrole macrocycle can be realized both by electrophilic and nucleophilic substitution reactions. 1,3-dithiolane as an umpolung formyl synthon, developed by Seebach and Corey [24], was used to insert formyl via nucleophilic addition of the corresponding lithium salt to the porphyrin. Senge investigated the reaction of the addition of 1,3-dithiane, deprotonated with *n*-butyllithium, in the presence of *N,N,N,N*-tetramethylethylenediamine (TMEDA), to porphyrins [23]. The products of the nucleophilic addition of the 1,3-dithianyl anion to the 5,15-diphenylporphyrin (DPP) **3**, 5,15,20-triphenylporphyrin (TrPP) **4**, and their nickel complexes (3Ni and 4Ni) were protonated, and the corresponding porphyrinogens were oxidized with DDQ. Subsequent deprotection of the formyl group was carried out with DDQ but in the presence of BF<sub>3</sub> etherate to give the corresponding *meso*-formyl DPP and TrPP derivatives **5** and **6** (Scheme 3). However, low yields and functional group intolerance of the method limit its use.



**Scheme 3.** Synthesis of *meso*-formylporphyrins via nucleophilic addition.

Takanami developed a more efficient and functional group-tolerant method of nucleophilic formyl group insertion using 2-(trimethylsilyl)pyridine. The reaction proceeded via nucleophilic addition of (2-pyridylmethylsilyl)lithium to DPP 3, followed by protonation of the intermediate anion and oxidation of the porphyrinogen back to the aromatic porphyrin ring to give DPP-CHO 5 (Scheme 4) [25,26]. It should be noted that mild oxidation of the *meso*-silyl porphyrinogen by air led to the *meso*-(hydroxymethyl)porphyrins 7 [27].



**Scheme 4.** Formylation with (2-pyridylmethylsilyl)lithium.

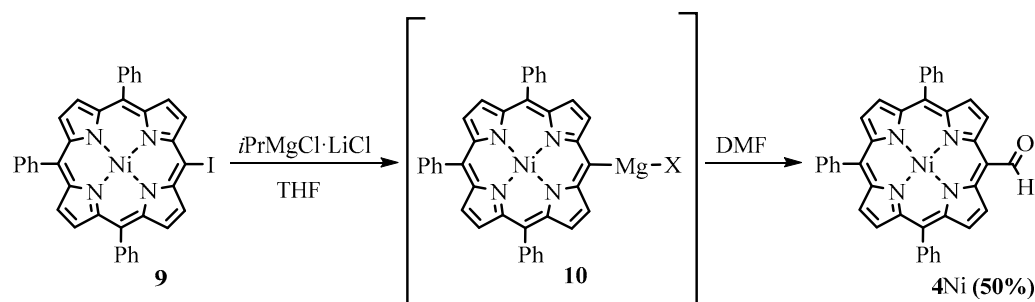
The reaction proceeds under mild conditions, and it is applicable to aryl- and alkyl-substituted porphyrins as well as their metal complexes. In addition to monoformyl derivatives, this method makes it possible to obtain diformyl derivatives, as well as more complex aldehydes with high yields. To confirm the mechanism, reactions were carried out with the addition of various electrophiles, such as acyl chloride, methyl chloroformate, isocyanates, and enones, resulting in the corresponding formyl derivatives 8, variously substituted at the opposite formyl *meso* position [28].

Osuka obtained porphyrin Grignard reagents for the first time using metal-iodine exchange between *meso*-iodoporphyrins and *i*PrMgCl. The utilization of the *meso*-magnesium-porphyrins in reaction with DMF led to the formation of the *meso*-formyl derivatives (Scheme 5) [29].

Reactions of electrophilic substitution have found the greatest application in the chemistry of porphyrins as electron-rich aromatics. More reactive *meso* positions are usually attacked by electrophiles. The electrophilic formylation can easily be performed using the Vilsmeier–Haack reaction. The synthesis of *meso*-formyl- $\beta$ -octaalkylporphyrins using Vilsmeier–Haack formylation was first reported more than half a century ago [30,31]. To

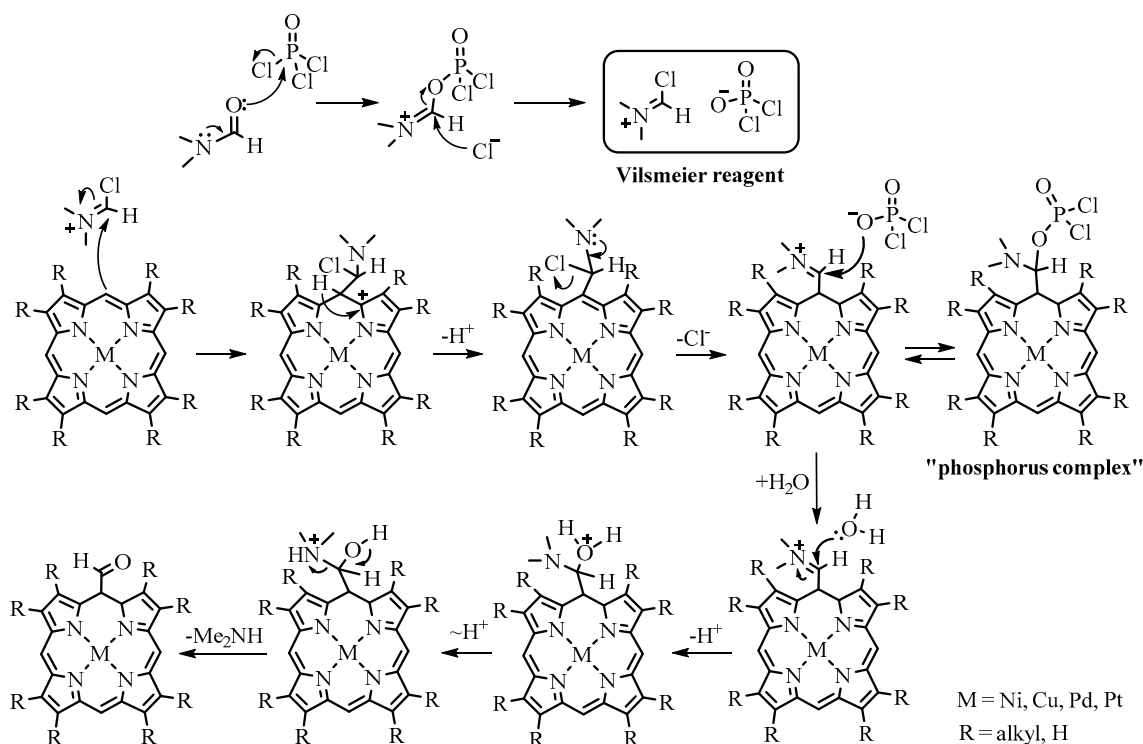


date, this reaction has become one of the most popular and efficient for obtaining *meso*-formylporphyrins.



**Scheme 5.** Formylation through the porphyrin Grignard reagent.

Porphyrin metal complexes resistant to HCl, released during the reaction, are substrates for formylate. It is known that the rate of formylation decreases with increasing electron acceptor ability of the metal cation in the series M(II) > M(III) > M(IV) and among M(II) in the series Ni(II) > Cu(II) > Pd(II) > Pt(II). Of the numerous variants of the reaction, the Vilsmeier reagent made from DMF/POCl<sub>3</sub> is usually used in porphyrin chemistry. The mechanism of the reaction is as follows: at the first stage, the electrophilic Vilsmeier reagent attacks the nucleophilic *meso* position of porphyrin, resulting in the formation of the iminium salt, which is the so-called “phosphorus complex”. Subsequent treatment of the phosphorus complex with water leads to the hydrolysis of the iminium salt, resulting in the formation of formylporphyrin (Scheme 6).

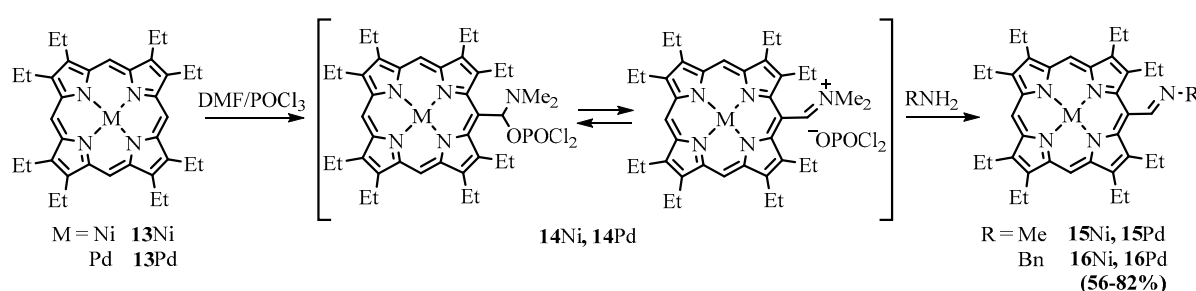


**Scheme 6.** Mechanism of the Vilsmeier–Haack formylation reaction.

## 2.2. Reactions of Meso-Formylporphyrins with Nitrogen Nucleophiles

Ponomarev investigated the Vilsmeier–Haack formylation of a number of Cu(II), Ni(II), and Pd(II) complexes of  $\beta$ -octaalkylporphyrins and chlorins and the subsequent transformations of the *meso*-formyl derivatives [5,32]. As an electrophile, the formyl group can react with a variety of nucleophiles, including organometallic reagents, CH-acids,

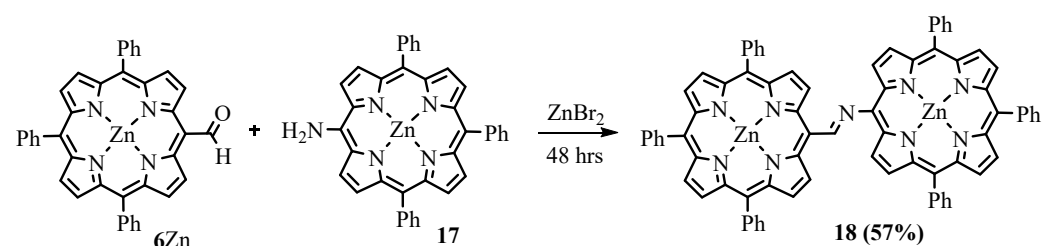
heteroatom nucleophiles (amines, thiols), electron-rich aromatic cycles, and heterocycles. The reaction of formylporphyrins with amines leads to azomethines or Schiff bases, and the corresponding studies up to the mid-1990s were summarized in the review of Ponomarev [20]. *Meso*-formyl porphyrins react with amines to give the corresponding imines; hydroxylamines give oximes; and hydrazines produce hydrazones. The Vilsmeier–Haack formylation of  $\beta$ -octaalkylporphyrin **13** produces the stable phosphorus complex **14** due to the sterical hindrances retarding hydrolysis of the complex. Ponomarev isolated phosphorus complexes of various porphyrins and used them instead of formylporphyrins for the preparation of Schiff bases [20]. The iminium group of the phosphorus complex is more active to nucleophilic attack compared to the formyl group. Azomethine derivatives of nickel and palladium complexes of various porphyrinoids, including OEP, tetraalkyl esters of coproporphyrins I and II, mesoporphyrin IX, and mesochlorin e6, were obtained by direct interaction of “phosphorus complexes” with amines (Scheme 7) [33–35].



**Scheme 7.** Preparation of azomethine derivatives of metal complexes of OEP (MOEP) from the intermediate phosphorus complex obtained from formylation of MOEP.

Azomethine substitution at the *meso* position noticeably shifts the UV-Vis absorption spectra of porphyrins to long wavelengths, thus making their metal complexes potential photosensitizers [34]. Schiff bases also impart basic properties to the porphyrins, and the corresponding Pt(II) and Pd(II) complexes of azomethine derivatives of OEP and tetramethyl coproporphyrin I were investigated as sensor dyes for measuring proton and oxygen concentrations using an optical noninvasive method [36,37]. The corresponding phosphorescent probe, based on the Pt(II) complex of *meso*-(*N*-methylimino)-OEP for cellular diagnostics using dual oxygen and pH measurements in living cells, has been reported [38].

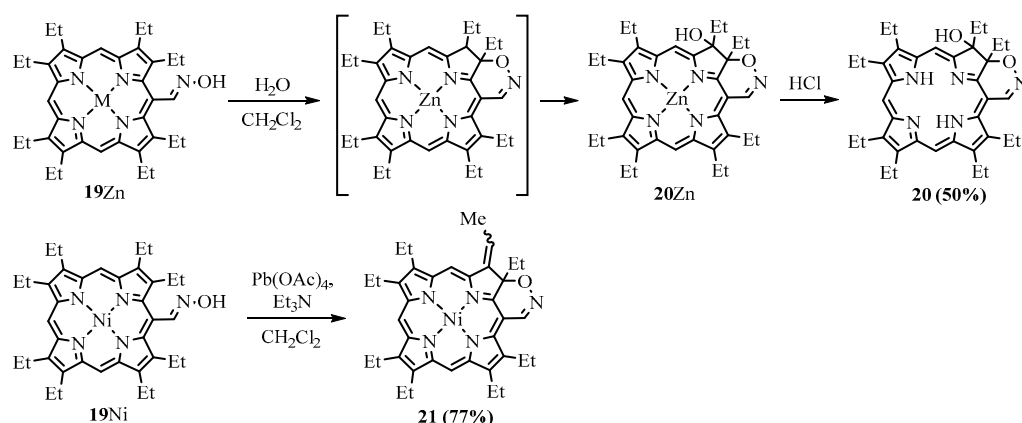
The imino group, which can be obtained by interacting the formyl group with an amine, was used as a linker to bond two tetrapyrrole chromophores into a dyad. The interaction of Zn(II) complexes of *meso*-formyltriphenylporphyrin **6Zn** and *meso*-aminotriphenylporphyrin **17**, catalyzed by Lewis acid  $\text{ZnBr}_2$ , led to the corresponding dimer of TrPP **18** (Scheme 8) [39]. The TrPP macrocycles are not coplanar in dimer **18** and consequently not conjugated. Nevertheless, there is some interchromophore communication, and dimer **18** features increased two-photon absorption, which can be used in PDT, providing deeper and more targeted treatment [40].



**Scheme 8.** Synthesis of the TrPP dimer bridged with the imino group.

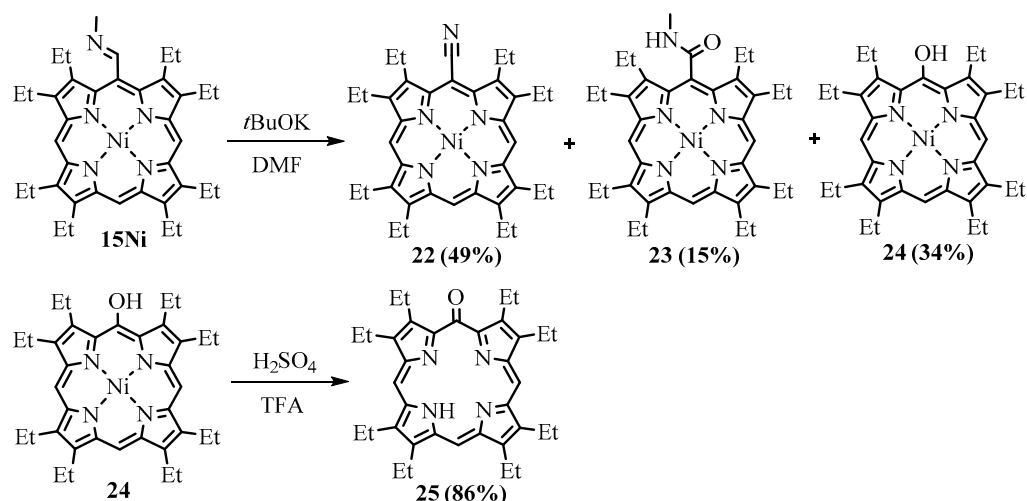
Schiff bases are useful synthons, as they can be subjected to further transformations. Elimination of *meso*-oximes led to *meso*-cyanoporphyrins [41]. Intramolecular cyclization

was observed when *meso*-oxime **19Zn** was vigorously stirred for a few hours in methylene chloride with a small amount of water. The probable intermediate chlorin with the fused 1,2-oxazin ring underwent hydroxylation via a peroxide mechanism to form stable hydroxychlorin **20Zn**. The use of an oxidant, lead tetraacetate, gave the product the same fused 1,2-oxazin but with a vinyl group instead of ethyl and hydroxyl (Scheme 9) [42,43]. Apparently, the difference between products **20** and **21** is in the water molecule, which was probably eliminated in the case of **21**. The UV-Vis spectra of the 1,2-oxazin annulated porphyrinoids **20** and **21** possess strong absorption bands in the red region.



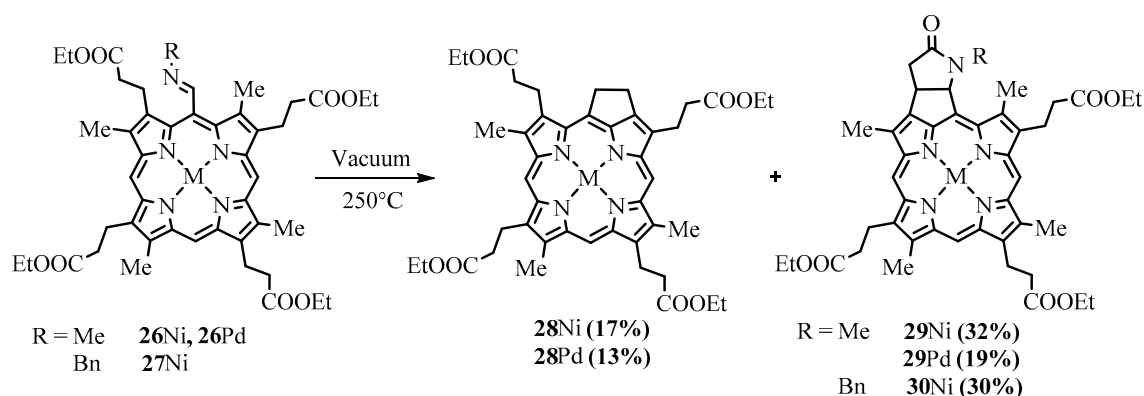
**Scheme 9.** Synthesis of porphyrinoids with fused 1,2-oxazin rings via oxime cyclization.

Treatment of the Ni(II) complex of *meso*-(*N*-methylimino)-OEP **15Ni** with *t*-BuOK led to the formation of the corresponding *meso*-nitrile **22**, *meso*-amide **23**, and *meso*-hydroxy **24** derivatives (Scheme 10). The latter was demetalated with sulfuric acid, resulting in phlorin **25** with strong light absorption in the region of 700 nm [35].



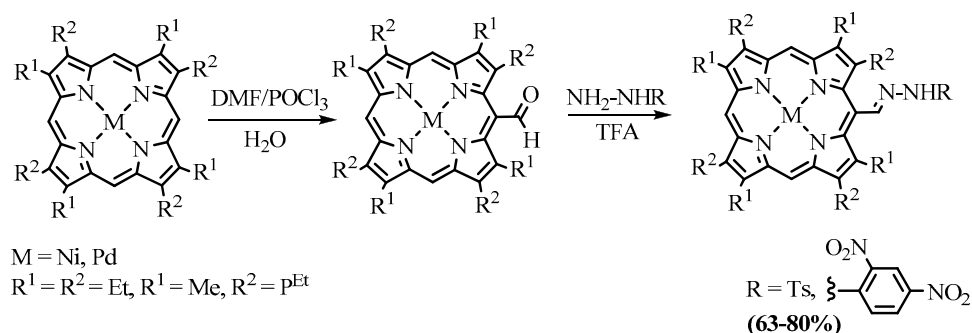
**Scheme 10.** Treatment of the *N*-methylimine derivative of NiOEP with *t*BuOK.

Thermolysis of *meso*-alkylimines of  $\beta$ -substituted metal porphyrins led to the formation of cyclopentane-fused derivatives (Scheme 11) [44–46]. The *meso*-imines of the tetraalkyl ester of coproporphyrin I (**26** and **27**) were transformed into a mixture of cyclopentane and cyclopentane-lactam bicycle fused derivatives (**28–30**) [35].



**Scheme 11.** Preparation of cyclopentane-annulated derivatives of coproporphyrins.

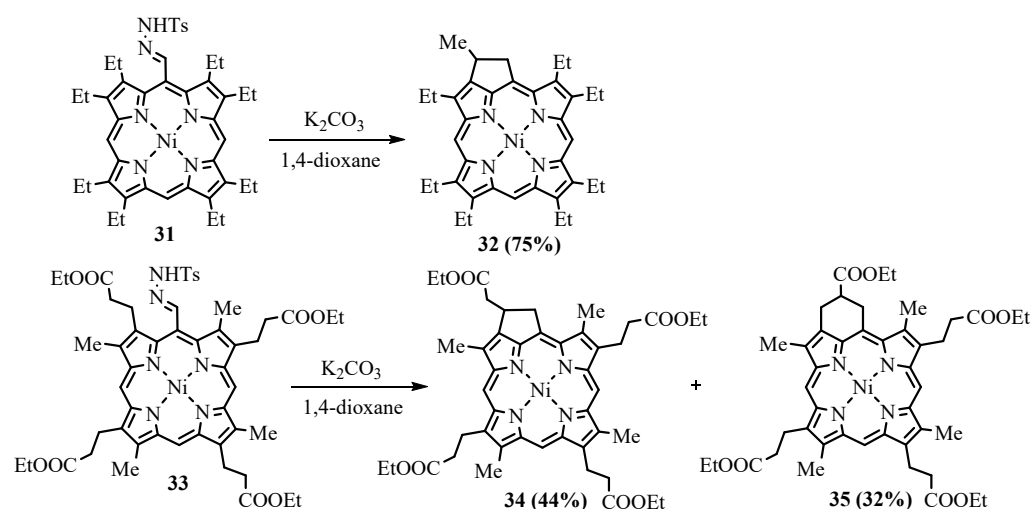
*Meso*-hydrazones of nickel and palladium complexes of OEP and coproporphyrin I ethyl esters were obtained as a mixture of *E*- and *Z*-isomers by the reaction of the corresponding *meso*-formyl derivatives with hydrazines catalyzed by trifluoroacetic acid (Scheme 12) [47].



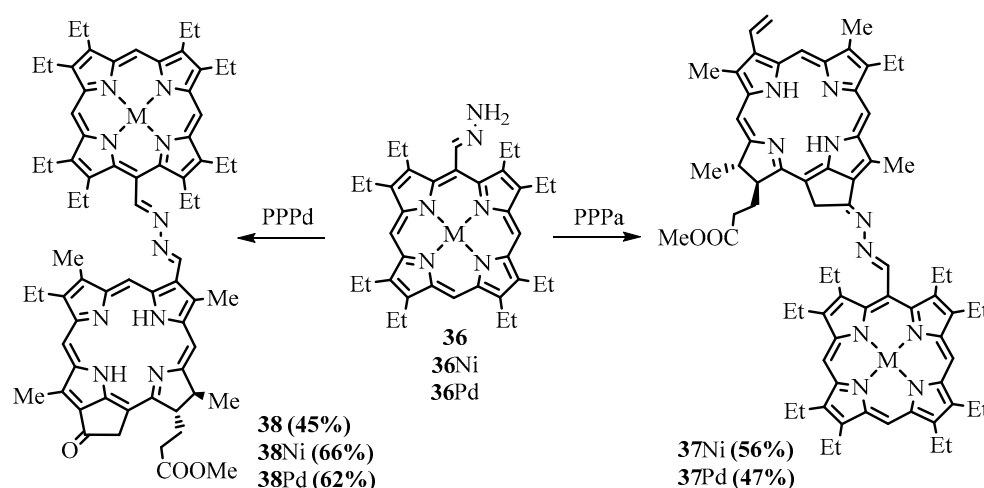
**Scheme 12.** Synthesis of hydrazones of metal complexes of OEP and coproporphyrin I.

*N*-tosylhydrazones **31** and **33** reacted with bases, generating an in situ porphyrin derivative of diazomethane, which released nitrogen molecules to give *meso*-carbene derivatives of porphyrins. Subsequent intramolecular insertion of the carbene into the CH bond of the neighboring  $\beta$ -substituent led to the corresponding fused cyclopentane (**32** and **34**) [48]. The cyclopentane fused products obtained were the same as in the thermolysis of azomethine **26**; however, the second product in the carbene-based reaction of **33** was cyclohexane fused product **35** instead of bicyclic lactam **29** obtained in the thermolysis of azomethine **26** [35], and yields of the products in the carbene-based cyclization were appreciably higher compared to the thermolysis (Scheme 13).

Unsubstituted *meso*-hydrazones of OEP **36** and also  $\beta$ -octaethylchlorin (OEC) were used in the preparation of dyads **37** and **38** bridged with the azine group [49]. Derivatives of the natural chlorins, methyl pyropheophorbide-*a* (PPPa) and methyl pyropheophorbide-*d* (PPPd), reacted with the *meso*-hydrazones of OEP and OEC, leading to the formation of the corresponding porphyrin-chlorin and chlorin-chlorin dyads (Scheme 14) [49]. Upon irradiation of the dyads, the energy of the excited state was efficiently transferred from the OEP (OEC) components to the pyropheophorbide chromophore. However, the chromophores weakly interacted in the ground state; therefore, the azine group was regarded as a conjugation switch, usually in the off state but capable of being turned on with a sufficiently strong driving force.



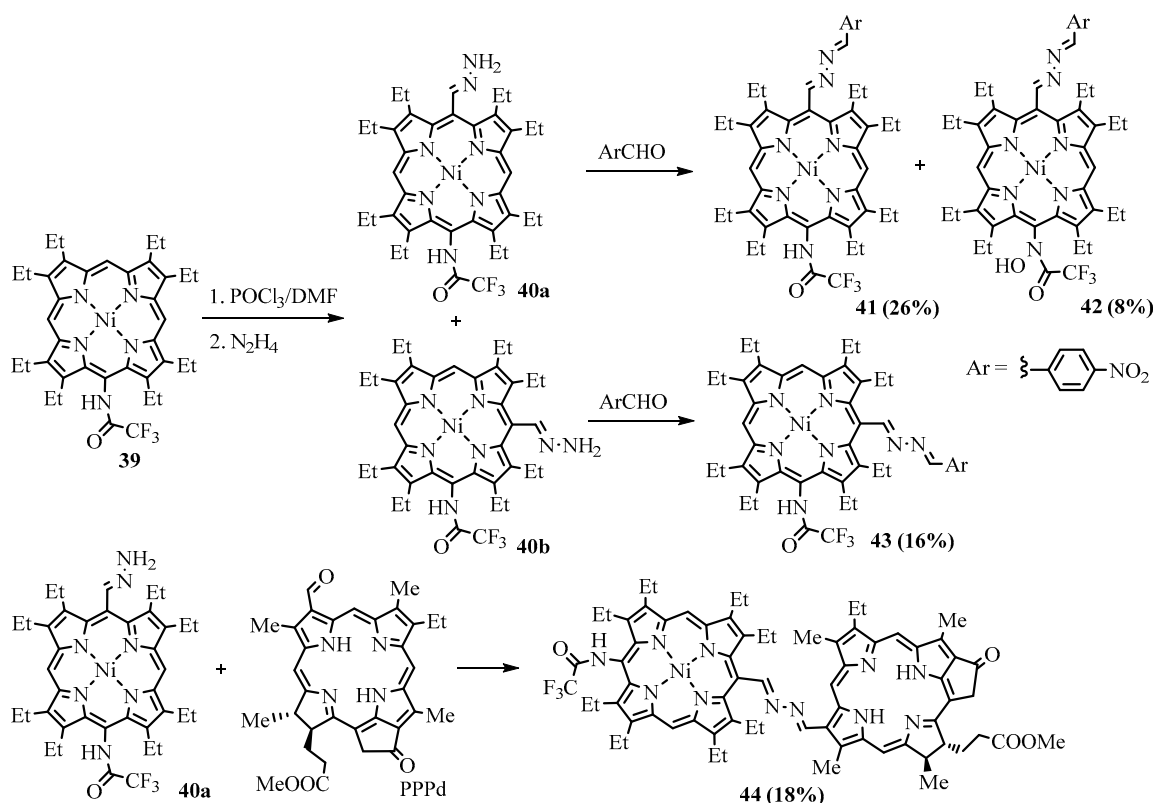
**Scheme 13.** Preparation of annelated porphyrins via intramolecular carbene CH insertion.



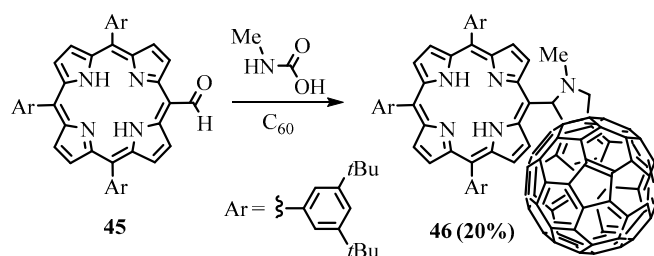
**Scheme 14.** Synthesis of dyads linked by the azine bridge.

One-pot *meso*-formylation, hydrazone, and azine formation were performed for *meso*-(trifluoroacetamido)-OEP **39** [50]. Under the conditions of formylation, the amide group was unexpectedly partially oxidized to form hydroxamic acid **42** (Scheme 15). The combined influence of trifluoroacetamide and arylazine groups in the products **41–43** led to strongly increased absorption near 500 nm and considerably red-shifted Q-bands up to 650 nm. Azine-bridged porphyrin-chlorin dyad **44** was obtained from *meso*-(trifluoroacetamido)-OEP **40a** and PPPd (Scheme 15). The dyad features substantial growth in the Q-band intensity as well as a red-shifting Soret band compared to the similar dyad without the trifluoroacetamido substituent.

The *meso*-formyl group of porphyrins can be transformed to azomethine ylide by interaction with *N*-methylglycine. 1,3-dipolar cycloaddition of the intermediate azomethine ylide to the double bond leads to porphyrins with *meso*-fused heterocycles. The porphyrin—fullerene conjugate **46** was obtained this way from *meso*-formyltriarylporphyrin **45**, *N*-methylglycine, and C<sub>60</sub> fullerene (Scheme 16) [18]. The irradiation of the dyad led to the formation of the exciplex due to the strong interaction between the porphyrin and C<sub>60</sub> chromophores at short distances.

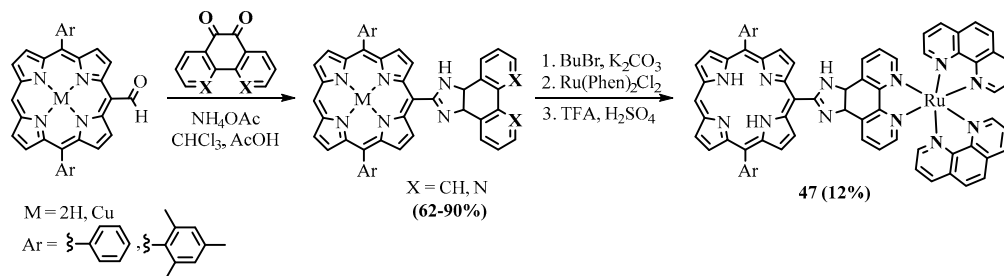


**Scheme 15.** Synthesis of  $\beta$ -octaethylporphyrin, oppositely substituted with trifluoroacetamide and azine groups.



**Scheme 16.** Synthesis of *meso*-linked porphyrin—fullerene conjugate.

Porphyrins functionalized with *meso*-fused 2-imidazolyl heterocycles were synthesized from the 5-formyl-10,20-diarylporphyrins and phenanthrene- or phenanthroline-5,6-dione in the presence of ammonium acetate (Scheme 17) [51]. The ruthenium phenanthroline complex of the free base porphyrin-imidazo[4,5-*f*]phenanthroline conjugate showed good binding ability to DNA and was capable of DNA photocleavage, which allows us to regard the complex as a potential photosensitizer for PDT [52].

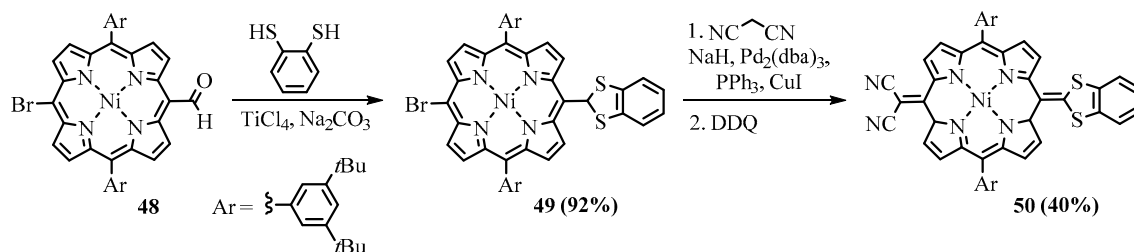


**Scheme 17.** Synthesis of porphyrins with *meso*-fused 2-imidazolyl heterocycles.



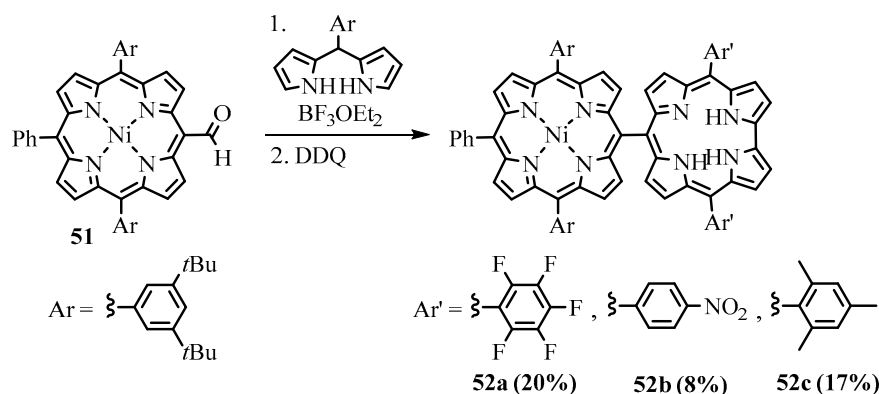
### 2.3. Reactions of Meso-Formylporphyrins with Miscellaneous Nucleophiles

A family of push-pull quinoidal porphyrins was obtained from a *meso*-formyl porphyrin **48** through the attachment of 1,3-dithiolane (benzo-1,3-dithiolane) and malononitrile fragments at the opposite *meso* positions of the 5,15-diarylporphyrin (Scheme 18) [53].



**Scheme 18.** Synthesis of porphyrins with *meso*-fused 2-imidazolyl heterocycles.

Directly linked porphyrin-corrole dyads **52a–c** were formed during condensation of the *meso*-formyltriarylporphyrin **51** with dipyrromethane (Scheme 19) [54]. A similar corrole-porphyrin-corrole triad was obtained when the 5,15-bisformylporphyrin was placed into the reaction. The strong exciton coupling between closely placed chromophores and reversible energy transfer were shown to exist in the dyad [55]. Directly *meso-meso*-linked porphyrin dimers and oligomers were obtained using condensation of *meso*-formylated porphyrins with pyrrole [21]. Such porphyrin dimers and oligomers were shown to act as prospective photosensitizers [56].



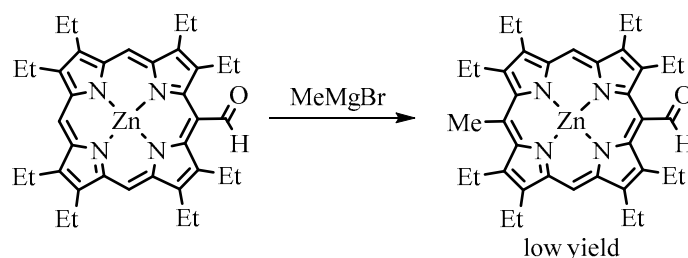
**Scheme 19.** Synthesis of porphyrin-corrole dyads.

### 2.4. Reactions of Meso-Formylporphyrins with Organometallic Reagents

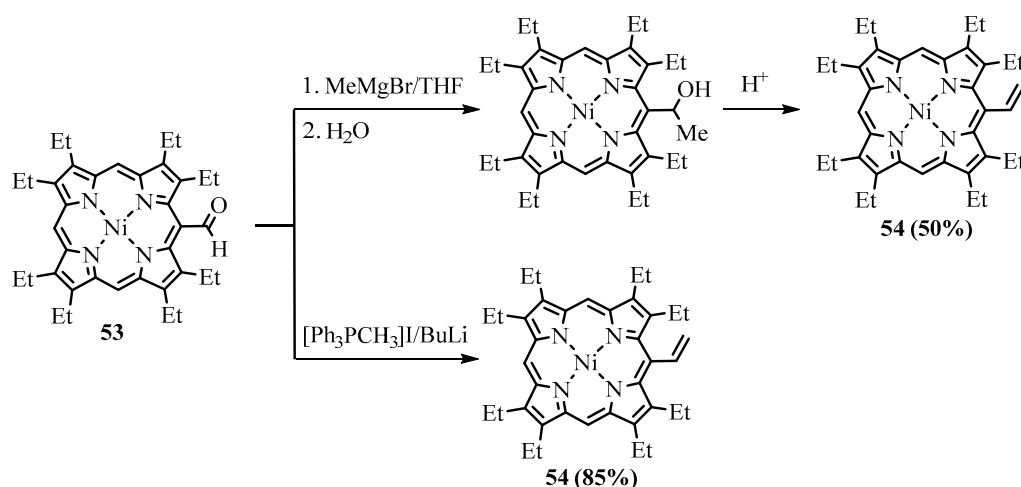
Among organometallic reagents, Grignard reagents were usually employed in the reactions for *meso*-formylporphyrins. Alkyl lithium reagents gave the expected products of addition to the carbonyl group only with less hindered  $\beta$ -formyl derivatives [15]. Grignard reagents interact with *meso*-formylporphyrins, leading to the formation of the corresponding secondary alcohols, but due to steric factors and perhaps other causes, this reaction proceeds somewhat slowly. Especially retarding is the presence of  $\beta$ -alkyl substituents. For example, Ponomarev reported the formation of the Mg complex of the formylporphyrin without significant formation of the target *meso*-(1-hydroxyethyl)-OEP upon treatment of *meso*-formyl-OEP (OEP-CHO) with MeMgI under heating [57]. Smith carried out a similar reaction with a free base of OEP-CHO and a Zn(II) complex of OEP-CHO (ZnOEP-CHO), which resulted in 15-alkylated products, and the formyl group remained intact (Scheme 20) [58]. However, when Johnson and Arnold used the Ni(II) complex of OEP-CHO in the same reaction, Ni(II) 5-(1-hydroxyethyl)-OEP was obtained, as expected [16]. Water was easily eliminated, yielding Ni(II) 5-vinyl-OEP **54** (Scheme 21). The Wittig reaction is cleaner and more efficient, as well as tolerating various functional groups such as

esters. Various Wittig reagents interacted with the *meso*-formyl group of  $\beta$ -substituted porphyrins to form *meso*-vinyl **54** (Scheme 21), 2-(ethoxycarbonyl)ethenyl **59**, 2-cyanoethenyl **56** (Scheme 22), and other alkenyl groups [5,14]. *meso*-formylporphyrins with *meso*-aryl groups without  $\beta$ -substituents were transformed to the corresponding *meso*-vinylporphyrins [59]. The products of the Wittig alkenylation can further be cyclized; for example, the methyl ester of coproporphyrin I was converted to the corresponding derivative of copropurpurin I **60** (Scheme 22). Purpurins and benzochlorins have an additional annealed cycle through *meso* positions and  $\beta$ -positions, which affect the  $\pi$ -electron system, leading to a bathochromic shift of the absorption bands. These annelated porphyrins and chlorins are more stable compared to other chlorins and have comparable electron-optical properties suitable for PDT. They have a higher efficiency than *meso* tetraphenylporphyrin and higher absorption in the longer wavelength region. The benzochlorins were shown to be of low dark toxicity towards Chinese Hamster ovary cells, whereas in the presence of light, total cell killing was observed at concentrations of the photosensitizer below 1  $\mu\text{g}/\text{mL}$  [60]. These promising properties of the annelated porphyrin derivatives attract the attention of medical researchers [61]. One of the representatives of this type of compound, tin etiopurpurin complex **64**, was used as a photosensitizer for PDT in human clinical trials. The drug was obtained from nickel etioporphyrin, which was formylated and reacted with a Wittig reagent, yielding *meso*-acrylate derivative **62**, which was cyclized in acid to give etiopurpurin **63**. The latter was metalated with tin(IV) chloride to give the drug for PDT (Scheme 23) [62]. The selectivity for the cyclization proceeding exclusively towards the carbon carrying the ethyl group vs. the carbon carrying the methyl group.

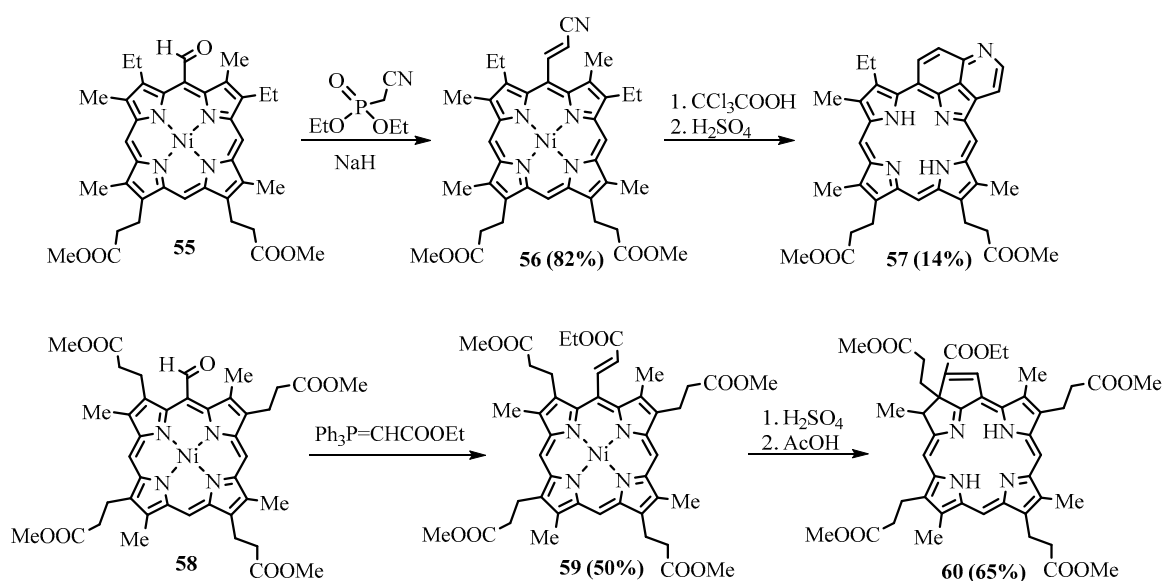
There are several published papers devoted to the synthesis of benzochlorin derivatives based on octaethylporphyrin and hematoporphyrin IX, as well as the study of their properties as photosensitizers [63–66]. In particular, the preparation of variously substituted benzochlorins containing fluorinated or alkyl groups has been reported [64].



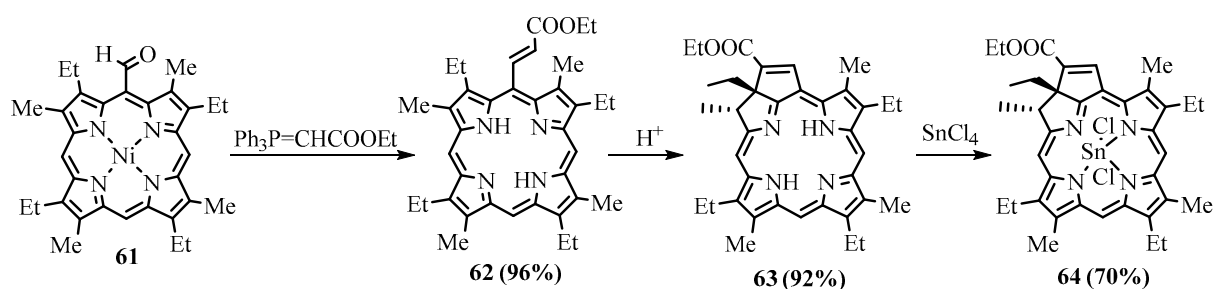
**Scheme 20.** The Grignard reaction of Zn(II) *meso*-formyl-OEP.



**Scheme 21.** The Grignard and Wittig reaction of NiOEP-CHO.

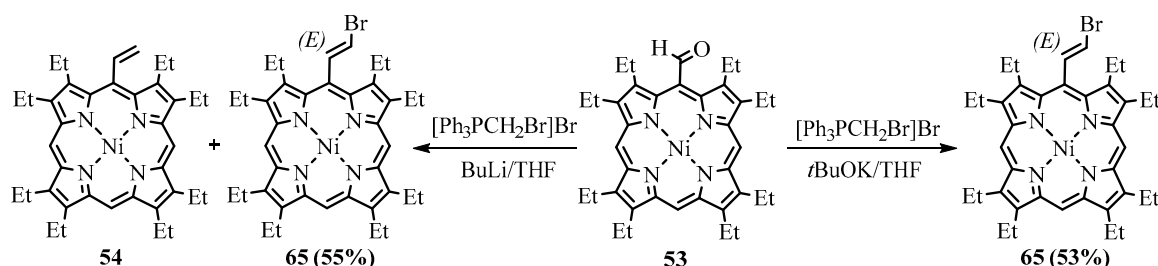


**Scheme 22.** Wittig alkenylation of Ni(II) complexes of methyl esters of *mesoporphyrin IX* and *coproporphyrin I* with subsequent cyclization.

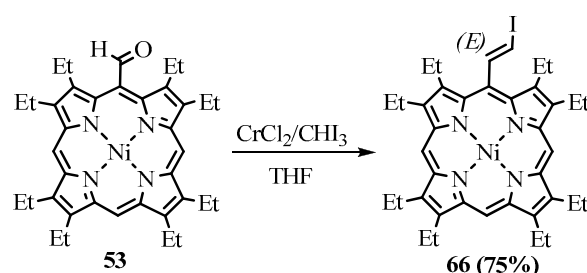


**Scheme 23.** Synthesis of the photosensitizer for the PDT tin(IV) etiopurpurin complex.

The formyl group can be transformed to the 2-haloethynyl group in one step using two different reactions. The Wittig reaction of NiOEP-CHO **53** with bromomethyltriphenylphosphonium bromide led to *meso*-(2-bromoethynyl)NiOEP **65** as a major (*E*)-isomer with a 55% yield [67]. However, the side metal-halogen exchange reaction led to the formation of lithiated methylene ylide and subsequently the formation of *meso*-vinyl byproduct **54**, which was hard to separate. The use of potassium *t*-butoxide in THF avoided contamination and produced a 53% yield (Scheme 24) [68]. Alternatively, the Takai reaction with iodoform catalyzed by CrCl<sub>2</sub> led to the formation of *meso*-(2-iodoethynyl)porphyrin **66** (Scheme 25). The obtained 2-haloethynyl derivatives were used as substrates of the cross-coupling reactions and precursors for the preparation of *meso*-ethynylporphyrins.

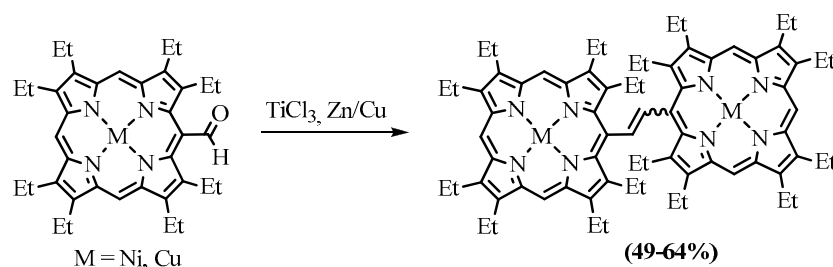


**Scheme 24.** Wittig bromoethenylation of NiOEP-CHO.



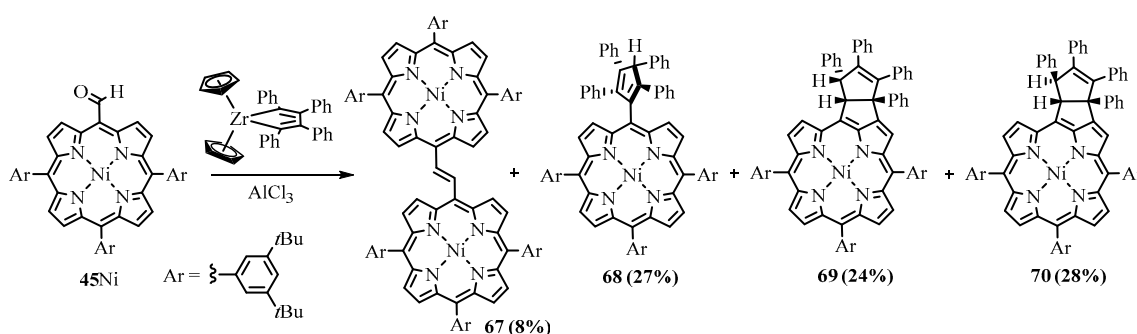
**Scheme 25.** Takai iodoethenylation of NiOEP-CHO.

Transformation of the formylporphyrins into dimers bonded with an ethene bridge can be performed using low-valent titanium, which is called the McMurry reaction [17]. Cu(II) and Ni(II) complexes of OEP-CHO were dimerized under the action of  $\text{TiCl}_3$  and Zn/Cu to form the corresponding complexes of dimers linked with the ethylene bridge in the form of a mixture of *cis* and *trans* isomers (Scheme 26) [69].



**Scheme 26.** McMurry dimerization of NiOEP-CHO and CuOEP-CHO [69].

The similar dimerization of the Ni(II) *meso*-formyltriarylporphyrin **45** Ni was observed as a side reaction of coupling with tetraphenylzirconacyclopentadiene in the presence of  $\text{AlCl}_3$ , along with products of cross-coupling: porphyrin—cyclopentene **69**, **70**, and cyclopentadiene **68** hybrids (Scheme 27) [70].

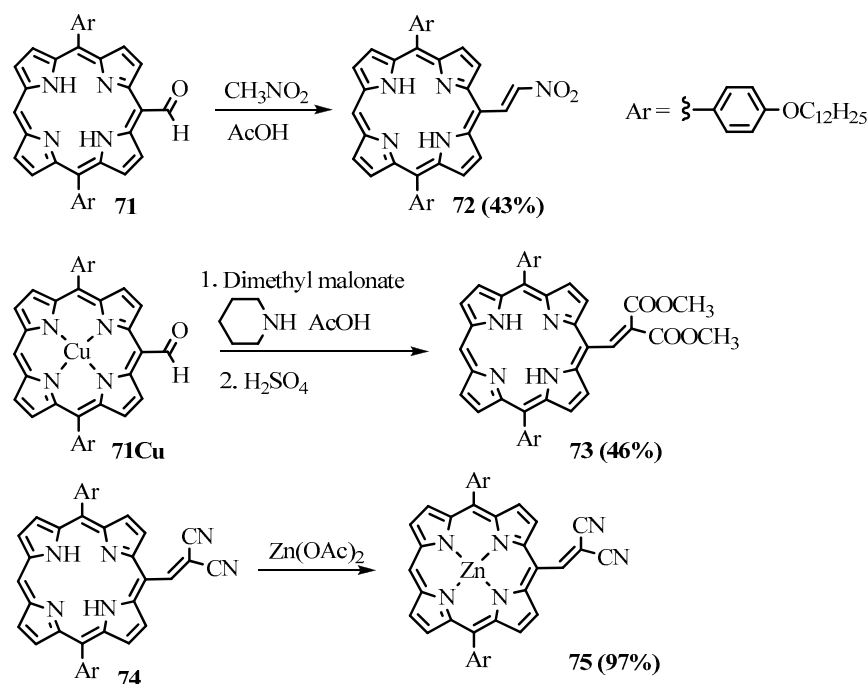


**Scheme 27.** Reaction of *meso*-formyltriarylporphyrin with tetraphenylzirconacyclopentadiene.

### 2.5. The Reaction of Meso-Formylporphyrins with CH Acids

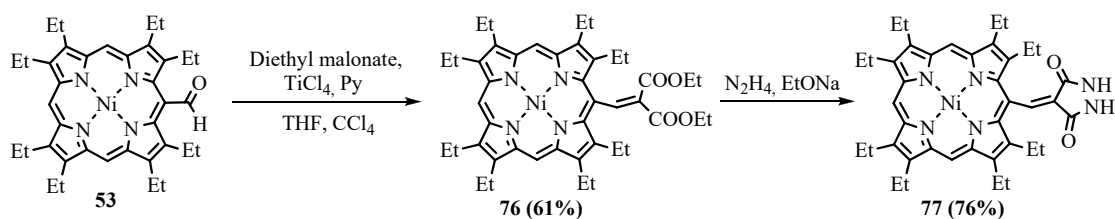
The Knoevenagel reaction allows for the transformation of formylporphyrins into the corresponding acrylic acid derivatives. The CH acid nucleophiles were introduced into the reaction with *meso*-formylporphyrins, leading to the formation of substituted *meso*-ethenyl porphyrin derivatives. *Meso*-formyl-diarylporphyrin **71** reacted with nitromethane, dimethylmalonate, and malononitrile in a mixture of piperidine, acetic acid, and toluene, leading to the corresponding substituted *meso*-(2-nitroethylene) **72** and *meso*-methylenemalonate **73** derivatives (Scheme 28) [71]. The *meso*-cyanoacrylate derivative **74** of Zn(II) *meso*-formyl-triarylporphyrin was obtained by heating in a mixture of piperidine and methanol for 16 h [72]. The product **75** of the reaction of *meso*-formyl-diarylporphyrin with malononitrile containing a *meso*-dicyanovinyl group was shown to act as a fluorescence “turn-on” cyanide probe [73]. The *meso*-nitroethylene derivative **72** was utilized as

fluorescence turn-on probes for biothiols as it exhibited fast fluorescence enhancement and high selectivity towards thiols based on the Michael addition mechanism [71]. It was also successfully applied to fluorescent cell imaging in the NIR wavelength range.

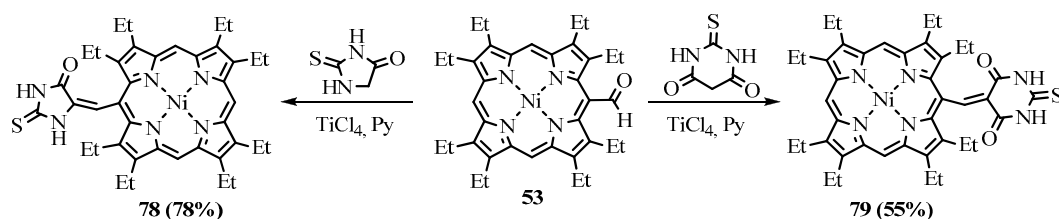


**Scheme 28.** The reaction of *meso*-formyldiarylporphyrin with CH acids.

NiOEP-CHO **53** was much less reactive in the Knoevenagel reaction compared to  $\beta$ -unsubstituted porphyrins due to the sterical hindrances and was gradually degraded under basic reaction conditions. In order to activate the formyl group against the attack of CH acid nucleophiles, Lewis acid  $\text{TiCl}_4$  was used in pyridine. The Lewis acid promoted the Knoevenagel reaction of the NiOEP-CHO **53** with malonic ester and heterocyclic CH acids [19]. The heterocyclic derivatives of porphyrins **77–79** linked with an exocyclic  $\text{C}=\text{C}$  double bond were obtained both by cyclization of the Knoevenagel product **76** from the reaction with malonic ester (Scheme 29) and by the Knoevenagel condensation of formylporphyrin with thiohydantoin and thiobarbituric acid (Scheme 30) [74].



**Scheme 29.** Synthesis of the conjugate of NiOEP with pyrazolidine-3,5-dione.



**Scheme 30.** Synthesis of the conjugate of Ni(II) OEP with thiohydantoin and thiobarbituric acid.

The UV-Vis spectra of the heterocyclic conjugates contain new bands that arose from the interaction of the conjugated chromophores as well as bathochromically shifted original absorption bands. Particularly dramatic changes were observed in the UV-Vis spectrum of the porphyrin conjugate with thiobarbituric acid, which exhibited substantial absorption enhancement in the visible spectral range due to the considerable  $\pi$ -electron conjugation between tetrapyrrole and heterocyclic chromophores.

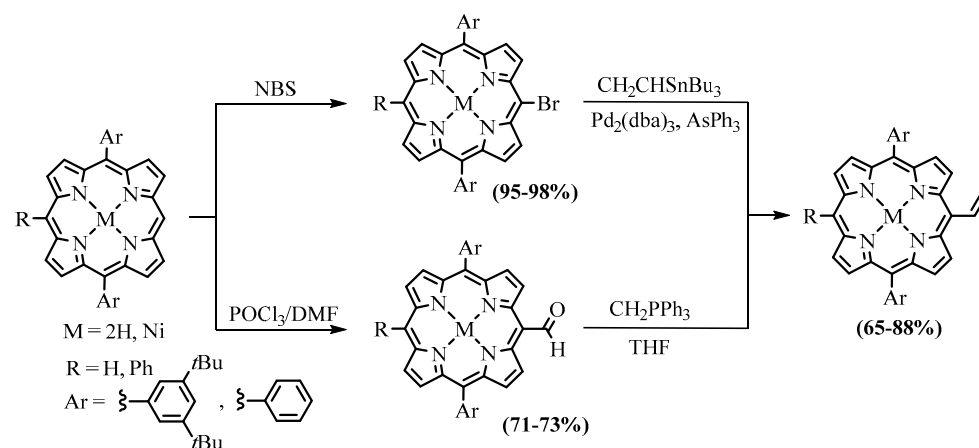
To sum up, *meso*-functionalization of porphyrins with the formyl group provides a powerful tool for the development of diverse porphyrin derivatives possessing valuable properties. In particular, promising photosensitizers with strong, red-shifted absorption bands, including NIR bands, were obtained from the *meso*-formyl porphyrins via the formation of annulated cycles such as benzochlorins and dibenzobacteriochlorins. *Meso*-imino derivatives were applied as sensor dyes in the multi-modal, multi-analyte optochemical sensing platform for cell diagnostics. Easily formed with the help of the formyl group, porphyrin conjugates with heterocycles can be used as biologically active compounds and in sensing applications. Imino- and azino-bridges represent two alternatives for bonding porphyrins into dyads, utilizing various pathways for energy transfer between the chromophores. Currently, the post-derivatization of the *meso*-formylporphyrins is under intense development.

### 3. Meso-Vinylporphyrins

Vinyl-substituted porphyrins are direct derivatives of formyl porphyrins, usually being obtained from the latter via the Wittig reaction. The vinyl group is a versatile nucleophilic synthon complementing electrophilic formyl. The electrophilic addition/substitution reactions and the modern catalytic cross-coupling and direct CH-functionalization methods are inherent to the vinyl group. The vinyl substituent can further be converted to the ethynyl group.

#### 3.1. Preparation of Meso-Vinylporphyrins

*Meso*-vinyl substituted porphyrins can be obtained from the *meso*-formylporphyrins using the Grignard and Wittig reactions as described in a previous section [14,16]. However, the efficient Vilsmeier–Haack porphyrin formylation reaction is limited to certain metal complexes and cannot be used for free bases or more labile zinc complexes. The alternative formyl preparation methods are based on palladium-catalyzed cross-coupling reactions, which are tolerant to other functional groups but require primary halogenation of the porphyrin core. Heck and Stille reactions with *meso*-bromoporphyrins led to the corresponding *meso*-alkenylporphyrins [59]. Starting *meso*-bromo derivatives can easily be obtained by bromination of *meso*-di(tri)arylporphyrins with NBS [75,76]. *Meso*-vinylporphyrins were synthesized from *meso*-bromoporphyrins by the Pd-catalyzed Stille reaction with vinyltributyltin (Scheme 31) [59,75,77].

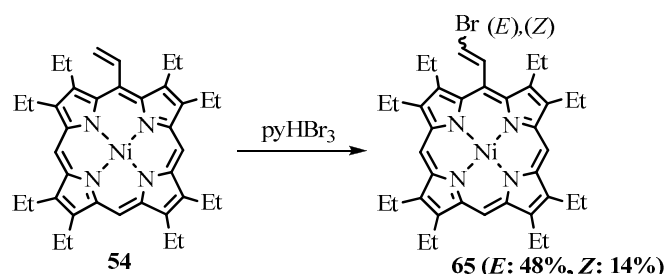


**Scheme 31.** Synthesis of the *meso*-vinylporphyrins.

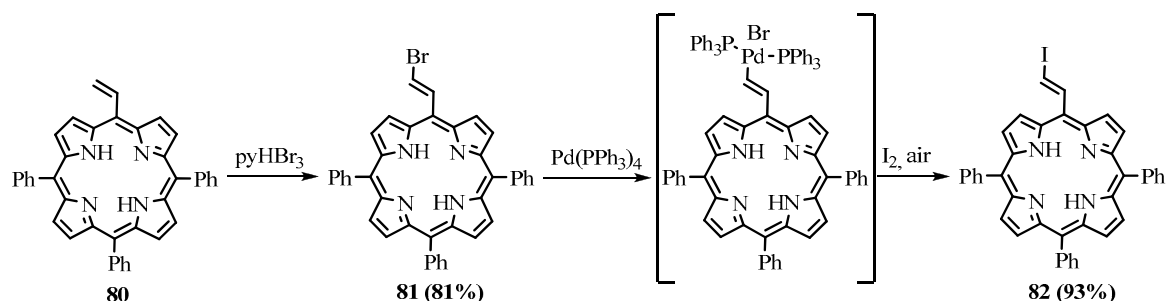


### 3.2. Transformations of *Meso*-Vinylporphyrins

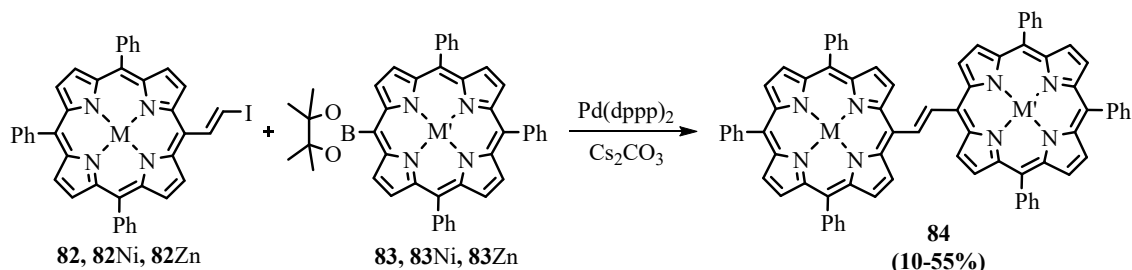
The carbon-carbon double bond of the vinyl group is susceptible to electrophilic addition. However, bromination of the *meso*-vinyl-NiOEP **54** with pyridinium tribromide led to the product of electrophilic substitution: the 2-bromoethenyl derivative **65** as a mixture of (*E*) and (*Z*) isomers (Scheme 32) [16]. Bromination of *meso*-vinyl-TrPP proceeded similarly [78]. Possibly, the sterical hindrances at the *meso* position hamper the second bromine atom addition. The bromination product *meso*-(2-bromoethenyl)porphyrin **65** can serve as a substrate in palladium-catalyzed cross-coupling reactions and as a precursor of *meso*-ethynylporphyrin. Cross-coupling of iodo derivatives proceeds easily, and this was the reason for the exchange of bromine for iodine via palladation/iodination (Scheme 33). The subsequent Suzuki coupling of the *meso*-(2-iodoethenyl)-TrPP **82** with *meso*-pinacolboronyl-TrPP **83** led to the TrPP dimer **84** being bridged by an ethene linker (Scheme 34) [78]. The dimer **84** exists in solution in a number of conformations differing in dihedral angles between the porphyrin and alkene planes. More coplanar conformers have appreciable  $\pi$ -electron conjugation and interchromophore interaction across the bridge.



**Scheme 32.** Bromination of *meso*-vinyl-NiOEP.



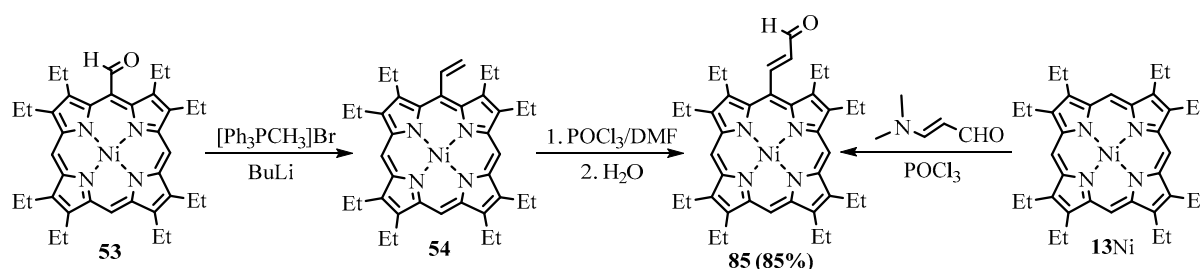
**Scheme 33.** Exchange of bromine by iodine via palladation/iodination.



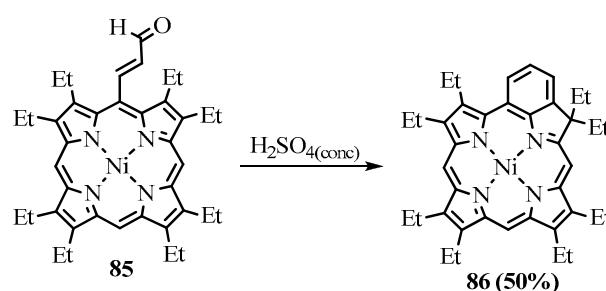
**Scheme 34.** Synthesis of TrPP dimer by Suzuki coupling of *meso*-(2-iodoethenyl)-TrPP with *meso*-bromo-TrPP.

The *meso*-vinyl group participated in electrophilic substitution reactions not only during bromination but also during formylation in Vilsmeier–Haack conditions. *Meso*-vinyl-NiOEP **54** was transformed to the corresponding *meso*-acroleinic derivative **85** by treatment with the Vilsmeier reagent DMF/ $\text{POCl}_3$  in 1,2-dichloroethane (Scheme 35) [79]. This compound can also be obtained using a short method by vinylogous formylation of

NiOEP **13Ni** with *N,N*-dimethylaminoacroleine/ $\text{POCl}_3$  [69]. The treatment of the *meso*-acroleine derivative **85** with concentrated sulfuric acid led to cyclization involving ethyl migration to give benzochlorin **86** (Scheme 36) [69,79].

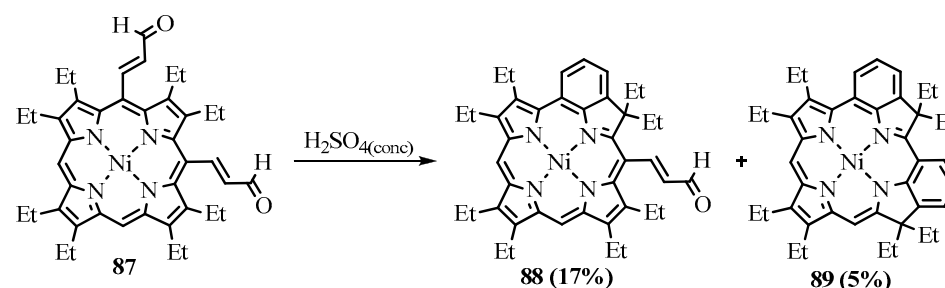


**Scheme 35.** Synthesis of *meso*-acroleine-substituted porphyrin.



**Scheme 36.** Synthesis of benzochlorin.

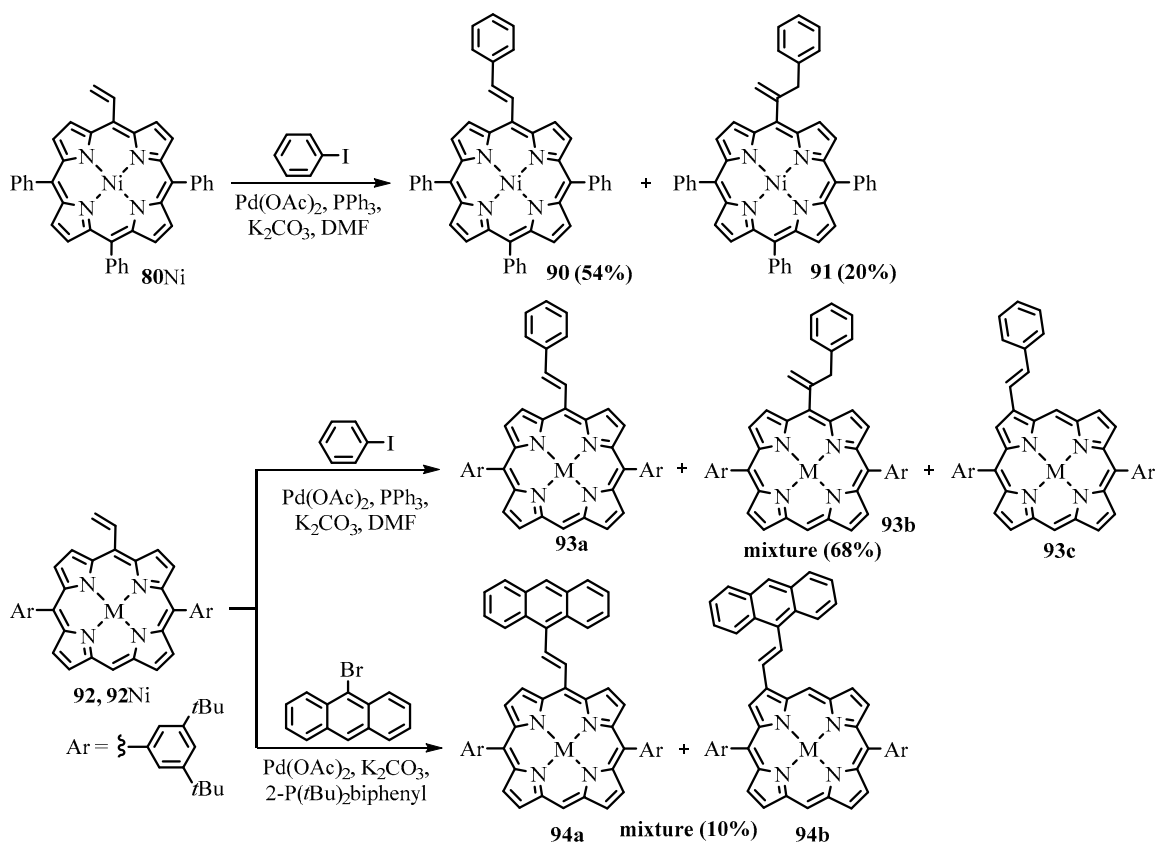
The octaethylbenzochlorin possesses significant red-light absorption, which makes it a potential photosensitizer for PDT [8,9,80,81]. Some benzochlorin derivatives can cause significant tumor regression at doses as low as 0.5 mg/kg body weight [82]. The product of the double cyclization of *meso*-bis-acroleinyl-OEP **87** is dibenzobacteriochlorin **89** [69], which possesses a strong absorption band in the region of 752 nm, thus fully corresponding to the tissue transparency window (Scheme 37) [8,82]. The conjugates of similar benzochlorin with carbohydrates were screened using the galectin-binding-ability assay and exhibited an enhancement of about 300–400-fold compared to lactose. All conjugates were also shown to possess good photosensitizing efficacy with fibrosarcoma tumor cells [65].



**Scheme 37.** Synthesis of dibenzobacteriochlorin.

Arnold studied the functionalization of porphyrins using the Heck reaction [59]. The Heck coupling of 5-vinyl-10,15,20-triphenylporphyrinatonicel(II) **80Ni** with 50 eq. iodobenzene was performed using a 20 mol%  $\text{Pd}(\text{OAc})_2$  catalyst with triphenylphosphine ligand  $\text{K}_2\text{CO}_3$  as a base in a mixture of DMF and toluene heated to 105 °C for 48 h. As a result of the reaction, two major regioisomers were formed: *trans*-1,2-disubstituted ethene **90** with a 54% yield and 1,1-substituted product **91** with a 20% yield. It should be noted that 1,1-substitution with a very bulky porphyrin substituent is not usual in the Heck reaction. However, an even more curious result was obtained in the reaction with

5-vinyl-10,20-diphenylporphyrinatonickel(II) **92Ni**, where additionally the  $\beta$ -substituted *E*-(2-phenylethenyl)porphyrin **94b** was formed (Scheme 38).

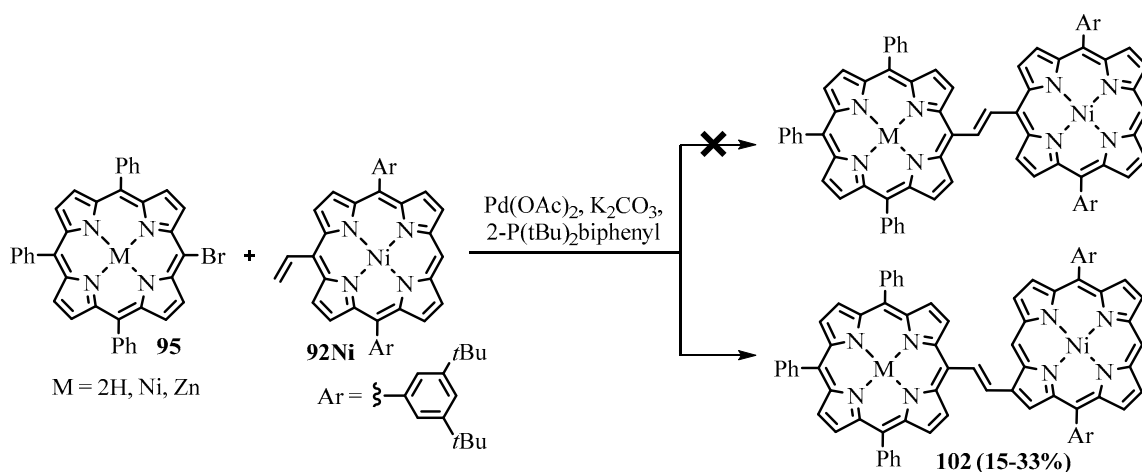
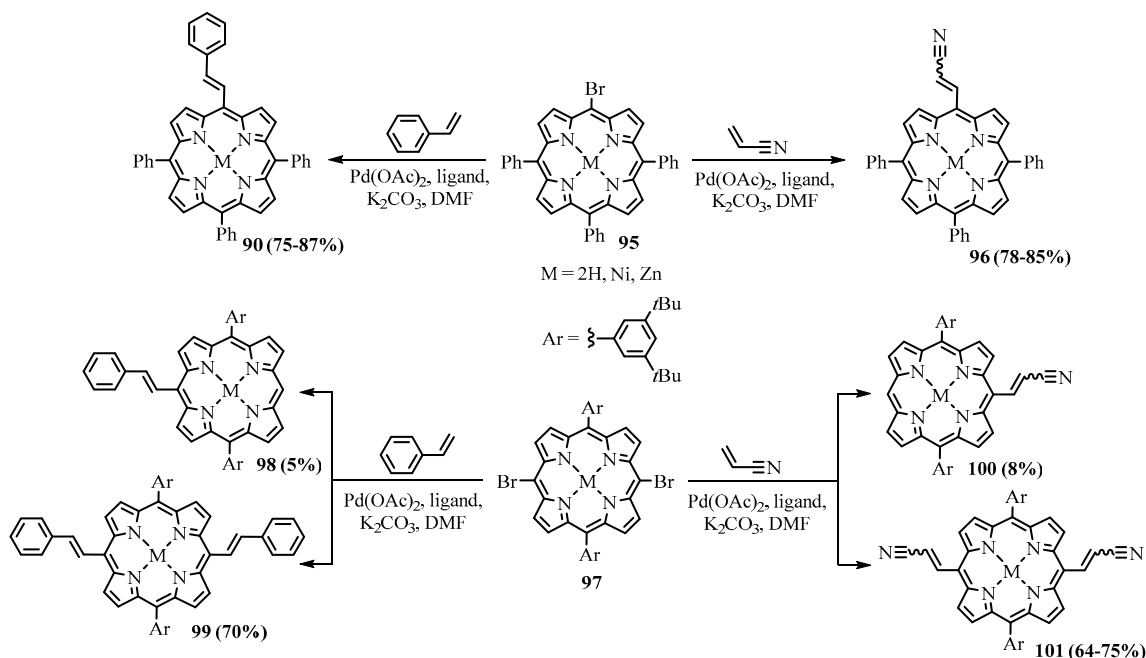


**Scheme 38.** Heck reactions of *meso*-vinylporphyrins.

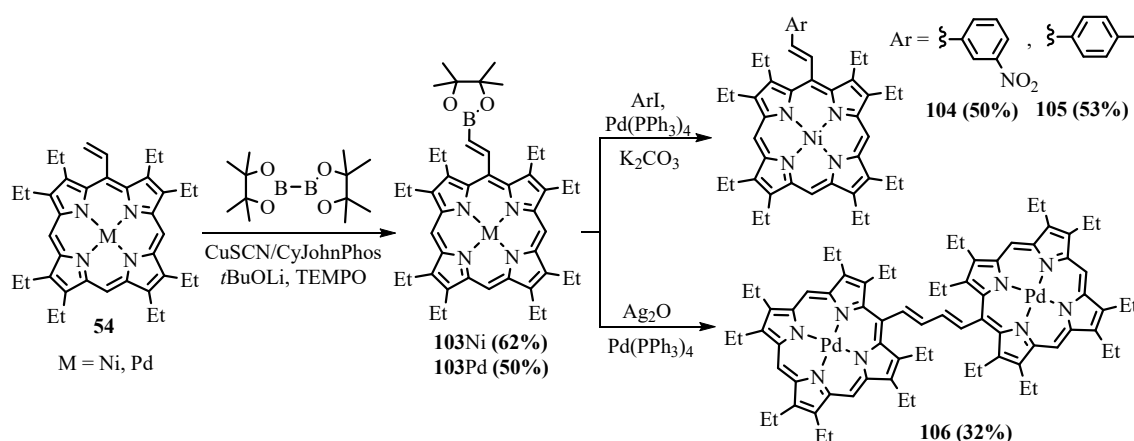
2-substituted ethenyl porphyrins were alternatively obtained using the Heck coupling of the *meso*-bromoporphyrins **95** and **97** with substituted ethene (usually with an electron acceptor group) [59]. The Heck coupling of 5-bromo-TrPP **95** and 5,15-dibromo-10,20-diarylporphyrin **97**, as well as their Ni(II) and Zn(II) complexes with large excesses of methyl acrylate, styrene, and acrylonitrile, led to the corresponding mono- and dialkenyl functionalized porphyrins (Scheme 39). *E*-isomers were obtained predominantly, but some amount of *Z*-isomer was also formed in the case of less sterically demanded acrylonitrile. Partial debromination was observed during the reaction. The free-base porphyrins were partially metalated with palladium. Zinc complexes were less stable compared to nickel complexes and were slightly demetalated and transmetalated.

The Heck reaction was used to produce a porphyrin dimer bound by ethene. However, a large excess of one substrate over the other cannot be used in coupling two porphyrin substrates, as was used in reactions with small molecules, because both coupling compounds are very precious. Consequently, the reaction was too slow, side reactions rose, and debromination of the bromoporphyrins occurred predominantly. The coupling of *meso*-bromo-TrPP **95** with *meso*-vinyl-diarylporphyrinatonickel **92Ni** did not give the target *meso*-ethenyl-linked dimer but rather *meso*,  $\beta$ -ethenyl-linked dyad **102** (Scheme 40). Free-base bromoporphyrin, Ni(II), and Zn(II) complexes gave the corresponding dyad yields of 23, 33, and 15%, respectively. The electronic absorption spectra of the dyads revealed a modest degree of interchromophore interaction via a partially conjugated bridge. This was explained by two factors: twisting of the ethene bridge at *meso* position with respect to the tetrapyrrole plane reduces  $\pi$ - $\pi$  conjugation, and linkage through the  $\beta$ -carbon has smaller orbital coefficients and consequently less influence on the  $\pi$ -electron system. The *meso*-*meso*-linked *meso*-arylporphyrin dimers

were obtained by several other transition metal-mediated methods: the Suzuki reaction of the *meso*-(2-iodoethenyl)porphyrin with *meso*-pinacolboronylporphyrin, described above [78]; the Stille coupling of 1,2-di(tributyltin)ethene with *meso*-bromoporphyrin [83]; *meso*-iodoporphyrin [39]; and the McMurry coupling of *meso*-formylporphyrin, described above in the formyl section [84].



The *meso*-vinyl group can also be functionalized via catalytic direct CH-functionalization reactions. The direct C-H borylation of the *meso*-vinyl group in NiOEP **54** was performed with Cu(II) complex as a catalyst, yielding the *meso*-(2-pinacolboronylethenyl)porphyrin **103Ni**, which was shown to act as a nucleophilic partner in the Suzuki cross-coupling leading to porphyrin derivatives **104** and **105** with an extended  $\pi$ -conjugation through the carbon double bond [85]. The oxidative homocoupling of the borylporphyrin **103Pd** produced the dimer **106** (Scheme 41) [86]. Thus, this strategy of *meso*-vinyl transformations allows for the attachment of various chromophores through the unsaturated bridges. The products of couplings possess some degree of conjugation across the bridge and interchromophore interaction, which induces a bathochromic shift of absorption bands.



**Scheme 41.** The borylation of the vinyl-porphyrin with the subsequent coupling reactions.

The *meso*-vinyl group in porphyrins differs in properties from  $\beta$ -vinyl and other vinyl-substituted aromatics. The sterical hindrances at the *meso* position decrease the reactivity of the vinyl group and change the results of reactions. For example, interaction with electrophiles led to electrophilic substitution instead of addition, like in aromatics. The Heck reactions proceeded harder. Probably, this was one of the reasons for quite a small amount of work devoted to the transformations of *meso*-vinyl groups, especially compared to the  $\beta$ -analogs. The rich potential of the *meso*-vinyl function is to be revealed.

#### 4. *Meso*-Ethyneporphyrins

Due to the absence of the sterically interacting extra substituents at the linking carbon, the *meso*-acetylenyl group is coplanar with the macrocycle ring and fully  $\pi$ -electronically conjugated to the tetrapyrrole aromatic system in contrast to other *meso*-attached unsaturated groups like vinyl, phenyl, etc. [87–91]. The acetylene linker has been shown to allow efficient  $\pi$ -conjugation and strong electronic communication between chromophores [92–94]. This advantage of the triple bond linker is used when one needs to create extended conjugated systems.

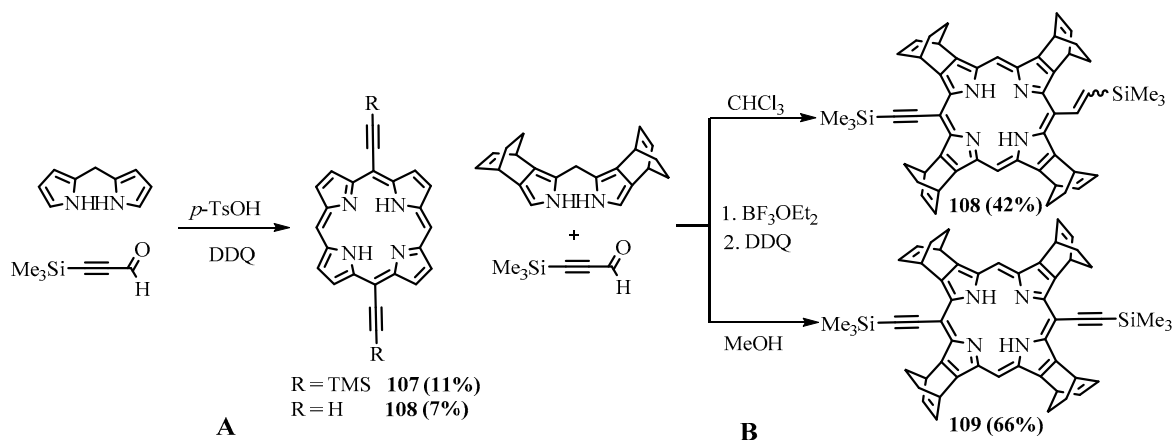
##### *Synthesis of Meso-Ethyneporphyrins*

There are several ways to obtain *meso*-acetylenylporphyrins, including classical functional group transformations and modern catalytic cross-coupling reactions. The oldest route utilized alkynyl-substituted precursors in the assembly of the porphyrin core. MacDonald [2 + 2] condensation of dipyrromethane with trimethylsilylpropynal led to the 5,15-bis(trimethylsilylethynyl)porphyrin **107** in 11% yield, which was deprotected and converted to the Ni(II) 5,15-bisacetylenylporphyrin **108** (Scheme 42A) [95]. In some cases, the product of the reduction of one triple bond can occur. 5-alkenyl-15-alkynyl-porphyrin **108** and 5,15-dialkynyl-porphyrin **109** were formed selectively depending on the choice of solvent (Scheme 42B) [96]. The alkenyl group arises from a protonation followed by intramolecular 1,2-hydride transfer from the methine position of porphyrinogen [96].

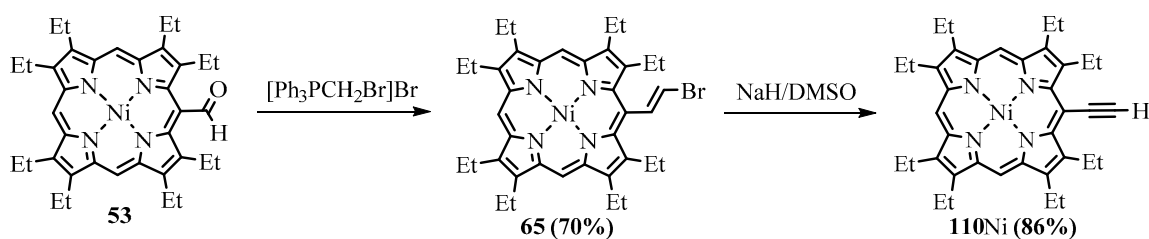
The classical way to obtain alkyne is through the elimination of hydrogen halide from halo-vinyl. The first *meso*-(2-bromoethenyl)-NiOEP **65** was obtained using the Wittig reaction of NiOEP-CHO **53** with bromomethyltriphenylphosphonium bromide. Then the Wittig product **65** was treated with dimsilyl sodium, yielding *meso*-acetylenyl-NiOEP **110**Ni with an 86% yield (Scheme 43) [95,97].

The most common way to insert an acetylenyl group into porphyrins is based on the Sonogashira reaction [97]. However, the Sonogashira reaction can be accompanied by some side reactions. The most common complication is the oxidative dimerization of the terminal alkynes [98]. Trialkylsilyl-protected acetylenes are often used, like trimethylsilyl- and triisopropylsilylacetylene, instead of gaseous acetylene, so the products are not able to dimerize. *Meso*-acetylenylporphyrin **112** was prepared in 82% yield by the Sonogashira coupling of

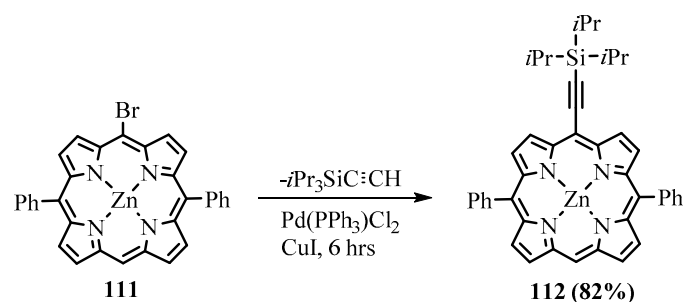
*meso*-bromo-porphyrin **111** with a 2.5 eq. excess of triisopropylsilylacetylene catalyzed by 20 mol% Pd(PPh<sub>3</sub>)<sub>2</sub>Cl<sub>2</sub> and 3 eq. CuI in THF with triethylamine (Scheme 44) [99].



**Scheme 42.** Synthesis of *meso*-acetylenylporphyrins via MacDonald [2 + 2] condensation of trimethylsilylacetylene and dipyrromethane (A); bicyclo[2.2.2]octadiene-fused dipyrromethane (B).

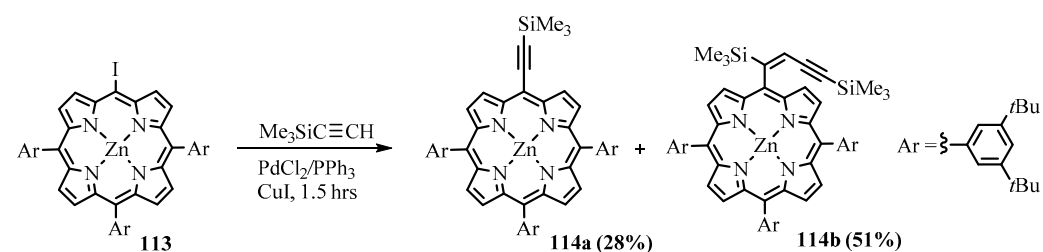


**Scheme 43.** Synthesis of *meso*-acetylenylporphyrin via elimination reaction.



**Scheme 44.** Synthesis of *meso*-acetylenylporphyrin via the Sonogashira reaction.

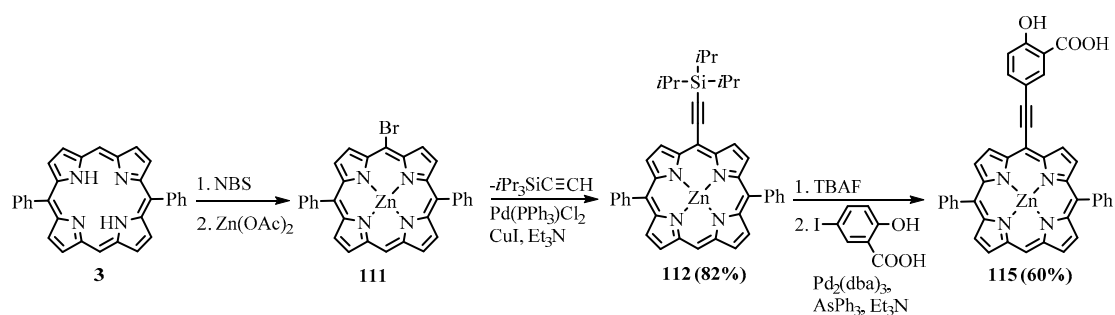
When the less bulky trimethylsilyl protection group instead of triisopropylsilyl was used in the Sonogashira reaction of 5-iodo-10,15,20-tris(3,5-di(*tert*-butyl))porphyrin **113** with an excess of trimethylsilylacetylene, the byproduct of the addition of the second acetylene molecule **114b** to the triple bond was obtained (Scheme 45) [100].



**Scheme 45.** The Sonogashira reaction was accompanied by a side reaction caused by the addition of the second acetylene molecule to the triple bond.

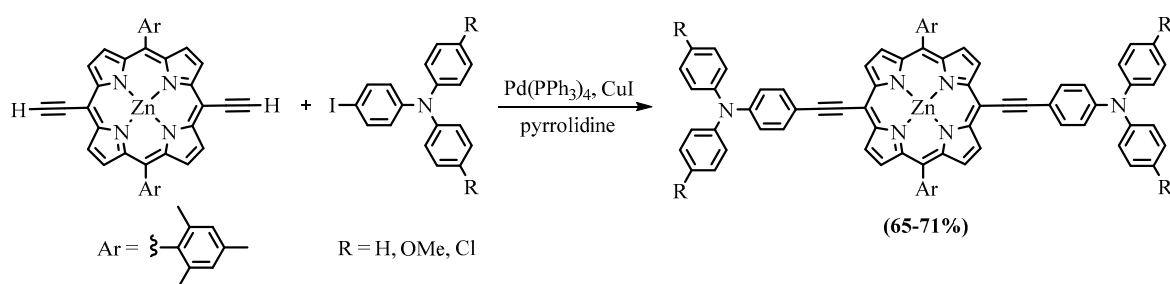


The most popular transformation of the *meso*-acetylenylporphyrins is also the Sonogashira coupling, leading to the triple bond linked dyad of the porphyrin with another fragment. Linking electron donors or acceptors to the porphyrin ring through the C≡C triple bond significantly affects the tetrapyrrole aromatic system. For example, to attach the salicylic acid anchor to the DPP **3**, the latter was first brominated at the *meso* position followed by zinc metalation and catalytic coupling with triisopropylsilylacetylene. Metalated porphyrins are usually applied as substrates in transition metal-catalyzed reactions instead of free bases to prevent scavenging of the catalytic metal by coordination with the macrocycle. Silyl protection is removed with TBAF, and the *meso*-acetylenyl porphyrin was next coupled with an iodo derivative of the salicylic acid, yielding the product **115**, with the anchoring group being conjugated to the porphyrin through the triple bond (Scheme 46) [99].



**Scheme 46.** Synthesis of *meso*-ethynylporphyrin and its transformation using consecutive Sonogashira reactions.

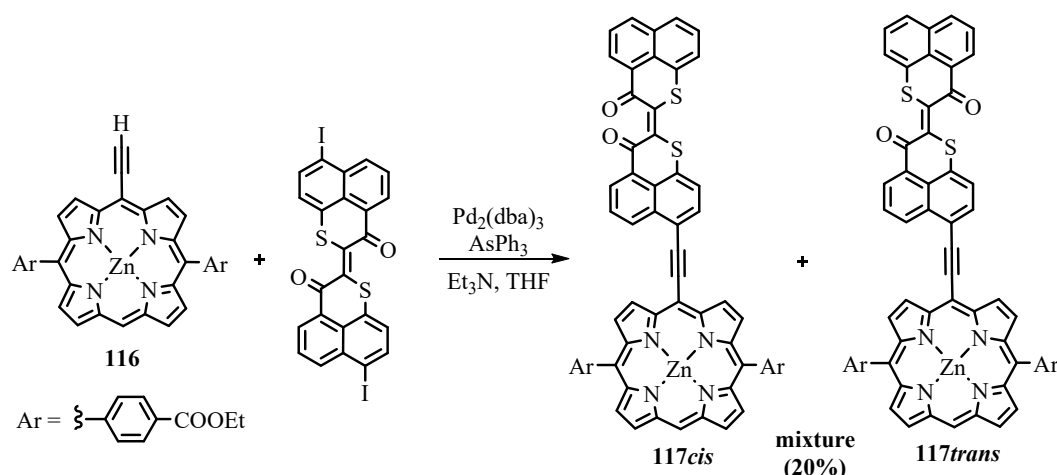
Strong electronic communication was observed between the triarylamine donors and porphyrin ring in the compound obtained by the Sonogashira reaction of *meso*-diacetylenylporphyrin with iodophenyldiarylamines (Scheme 47) [101]. The UV-Vis absorption spectra are considerably bathochromically shifted relative to the starting *meso*-arylethynylporphyrin and exhibit a broad Soret band and an intense Q band.



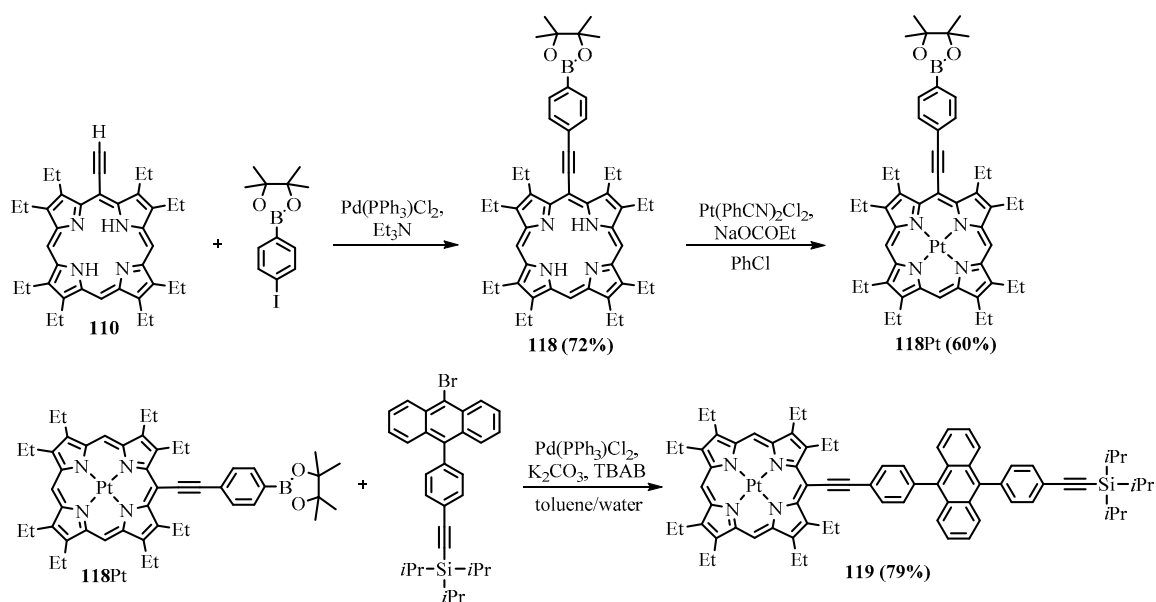
**Scheme 47.** Synthesis of porphyrin with triarylamine donors, linked by ethyne bridges.

With the help of Sonogashira coupling, a new photochromic porphyrin-perinaphthothioindigo dyad **117** was prepared (Scheme 48). One of the iodine atoms of the diiodoperinaphthothioindigo reagent was reduced during the reaction, which led to the predominantly mono-substituted product. A small amount of the bisporphyrin-substituted triad was also obtained. Due to the extended conjugated system, the dyad **117** exhibited efficient two-photon absorption properties and clear photochromic switching between *cis* and *trans* isomers [102]. The two photon absorption cross-section maxima for both isomers appeared around 850 nm, with values of 2000 GM for *trans* and 700 GM for *cis* isomers.

The dyad **119** of PtOEP with di(*p*-acetylenylphenyl)anthracene was obtained using Sonogashira and Suzuki coupling of the components. The efficient triplet energy transfer with nearly quantitative quantum efficiency was shown to proceed upon excitation from the porphyrin unit to the anthracene unit (Scheme 49) [103].



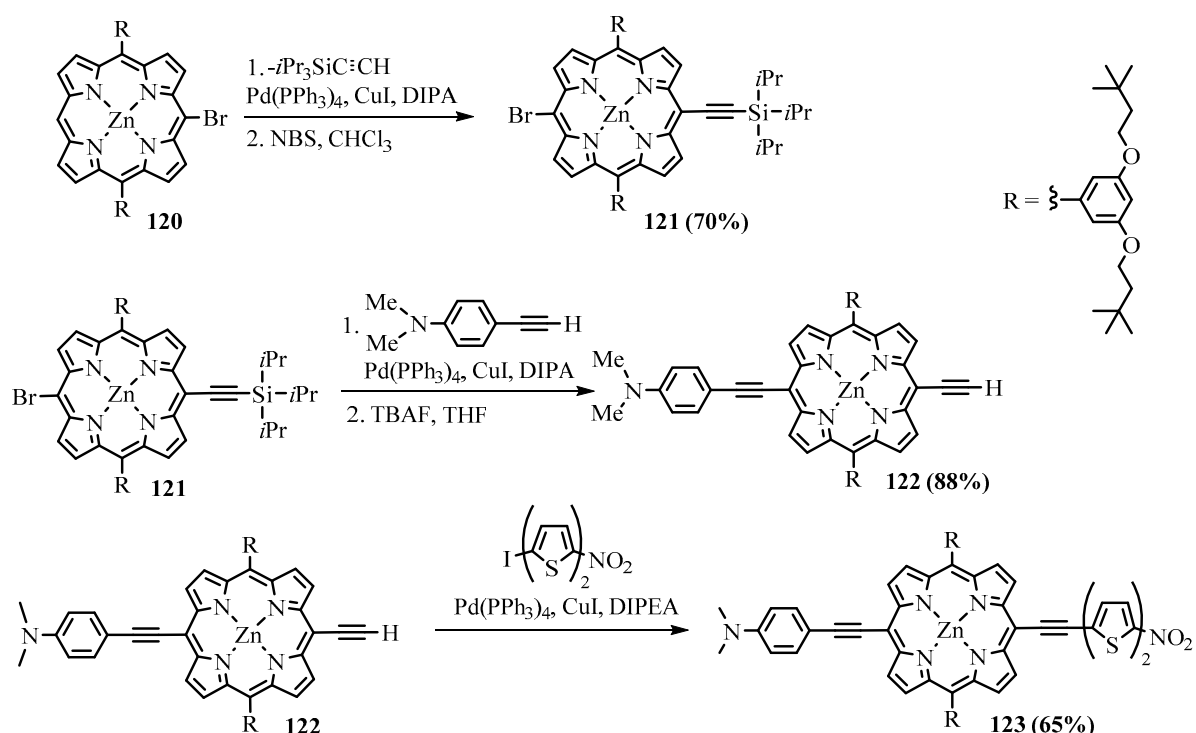
**Scheme 48.** Synthesis of the porphyrin-perinaphthothioindigo dyad.



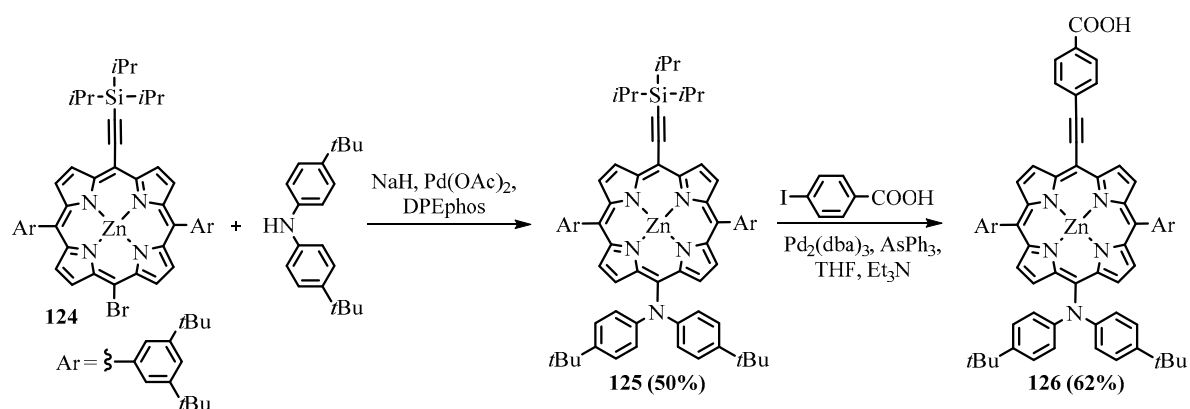
**Scheme 49.** Synthesis of the porphyrin-perinaphthothioindigo dyad.

Especially dramatic influence is exerted by so-called push-pull, both donor and acceptor substituted porphyrins. Electron donor *N,N*-dimethylaniline and electron acceptor nitrobisthiophene-substituted acetylenes were attached to the opposite positions of the porphyrin via Sonogashira coupling (Scheme 50). Such dipolar functionalized porphyrins possess considerable molecular hyperpolarizability and can be used for electro-optic applications [104,105].

Push-pull porphyrins have become the most efficient tetrapyrrole photosensitizers for dye-sensitized solar cells (DSSC). The dye with the donor diarylamino group and acceptor carboxyphenyl group, linked at the opposite *meso* positions with an ethyne bridge, outperformed all other porphyrins [106,107]. The synthetic strategy is similar to the examples given above. The Sonogashira coupling of *meso*-bromoporphyrin with trimethylsilylacetylene was carried out first, then the free *meso* position was brominated, followed by Buchwald amination with diarylamine, and after removing the trimethylsilyl protecting group, the second Sonogashira coupling with iodobenzoic acid was performed (Scheme 51).



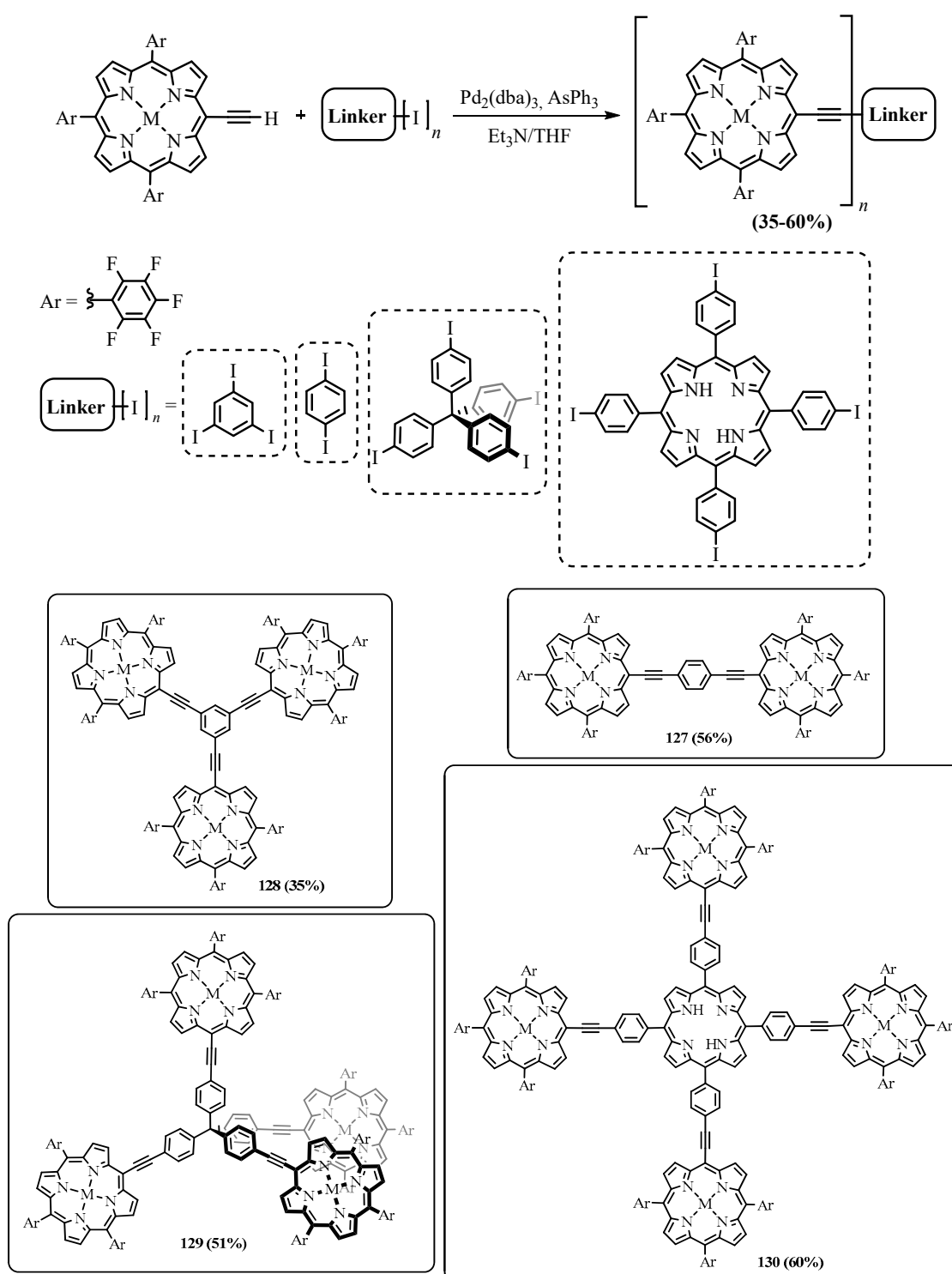
**Scheme 50.** Synthesis of push-pull substituted porphyrin with ethynyl linkers.



**Scheme 51.** Synthesis of the most efficient type of porphyrin sensitizer for DSSC.

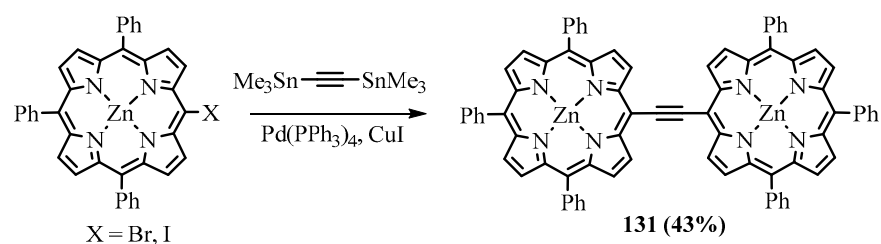
A large range of 5,15-bisalkynyl substituted porphyrin derivatives were obtained by Sonogashira coupling *meso*-dibromo-di(carboxyphenyl)porphyrins, which were shown to be suitable for the synthesis of surface-anchored MOF thin films [108].

The conjugated dimer and trimer with di- and triethynylbenzene bridges were obtained by the Sonogashira coupling of *meso*-ethynylporphyrin with di- and triiodobenzene. Whereas nonconjugated oligomers were obtained with tetrakis(4-iodophenyl)methane and tetrakis(4-iodophenyl)porphyrin (Scheme 52) [109]. Different types of oligomers with diphenylacetylene bridges were obtained as a result of the Sonogashira coupling of *meso*-(4-ethynylphenyl)porphyrin with *meso*-(4-iodophenyl)porphyrin [110] and *meso*-bis(4-iodophenyl)porphyrin [111]. It is worth noting that the directly attached aryl group at *meso* position is not conjugated with the macrocycle because it turned almost perpendicular owing to the sterical interactions, and the dimers linked through the *meso*-phenyl [112], including the *meso*-diphenylacetylene bridge [111], are not conjugated [113].



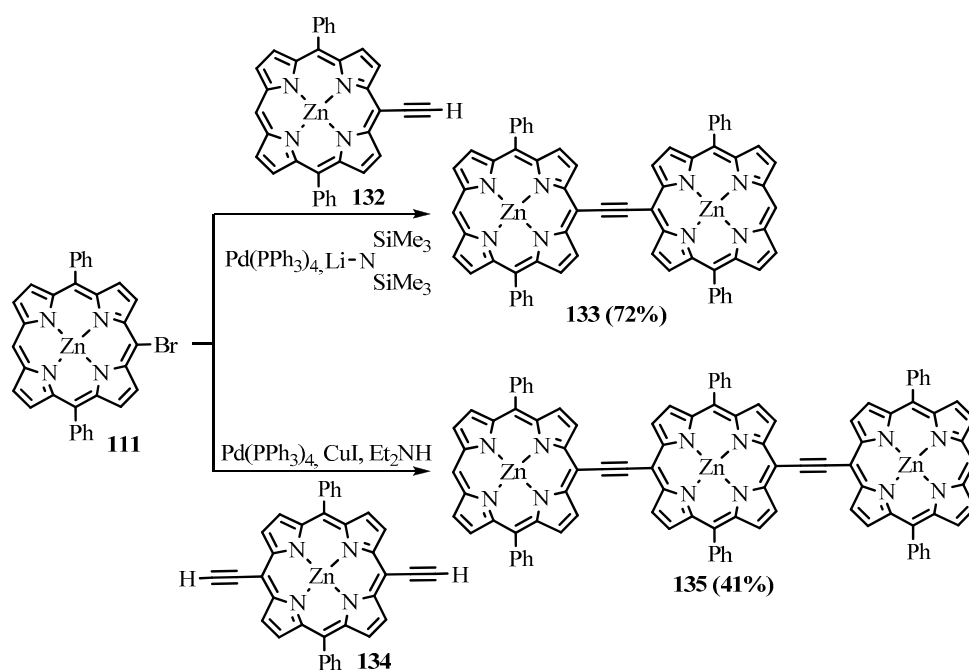
**Scheme 52.** Synthesis of conjugated porphyrin dimer and trimer with ethynylbenzene bridges using Sonogashira coupling.

The fully conjugated porphyrin dimer **131**, directly linked by acetylene at *meso* position was obtained using Stille-type coupling of bis-1,2-stannylacetylene with 5-halo-TrPP with a 43% yield (Scheme 53) [39]. The electron absorption spectrum of the dimer **131** showed considerable changes compared to the monomer, which can be attributed to the extensive conjugation and strong interchromophore communication.

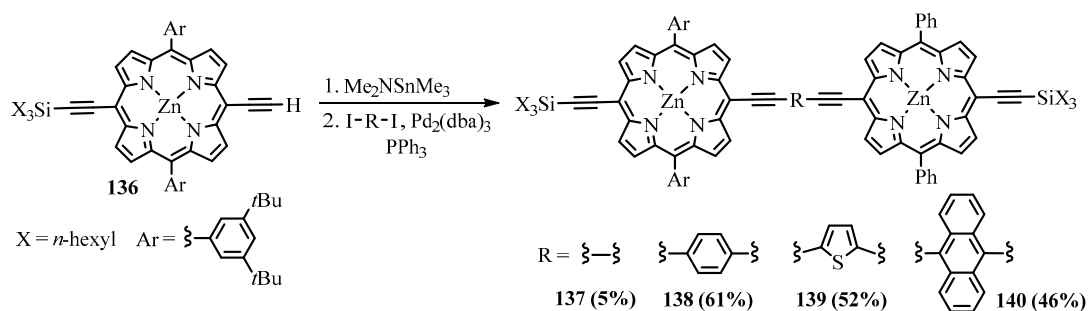


**Scheme 53.** Synthesis of porphyrin dimer with ethynyl bridge using Stille coupling.

The DPP dimers and trimers bridged by ethyne linkers were obtained by the Sonogashira coupling of *meso*-ethynylporphyrin **132** and **134** with *meso*-bromo-porphyrin **111** (Scheme 54) [92]. The dimers with diethynylarene bridges **137–140** were obtained by the Sonogashira coupling of partially protected *meso*-diethynylporphyrin **136** with diiodoarenes (Scheme 55) [114]. The thiophene linker provided more conjugation than phenylene but less than anthracene, which allowed even more electronic communication than the simple butadiyne. All *meso*-arylporphyrin dimers with triple bond linkers possess high cross-sections of two-photon absorption, which makes them the most promising candidates for photosensitizers in two-photon-induced PDT. Efficient singlet oxygen generation was demonstrated both in one- and two-photon excitation of these dimers [115].

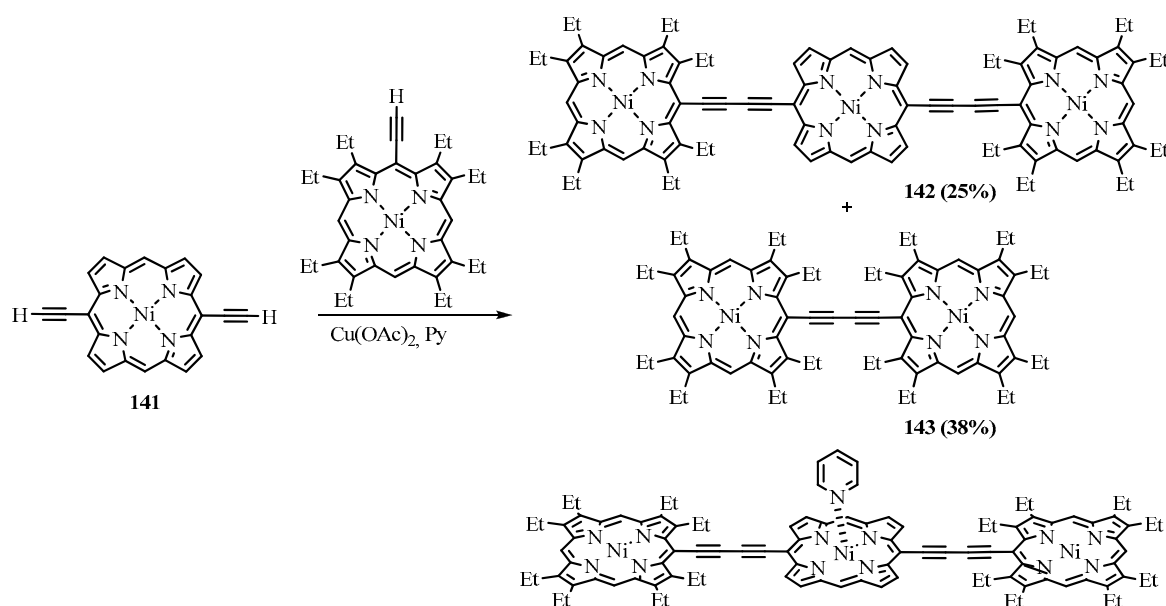


**Scheme 54.** Synthesis of porphyrin dimer and trimer with ethyne bridge using Sonogashira coupling.



**Scheme 55.** Synthesis of porphyrin dimer and trimer with diethynylarene bridges using Sonogashira coupling.

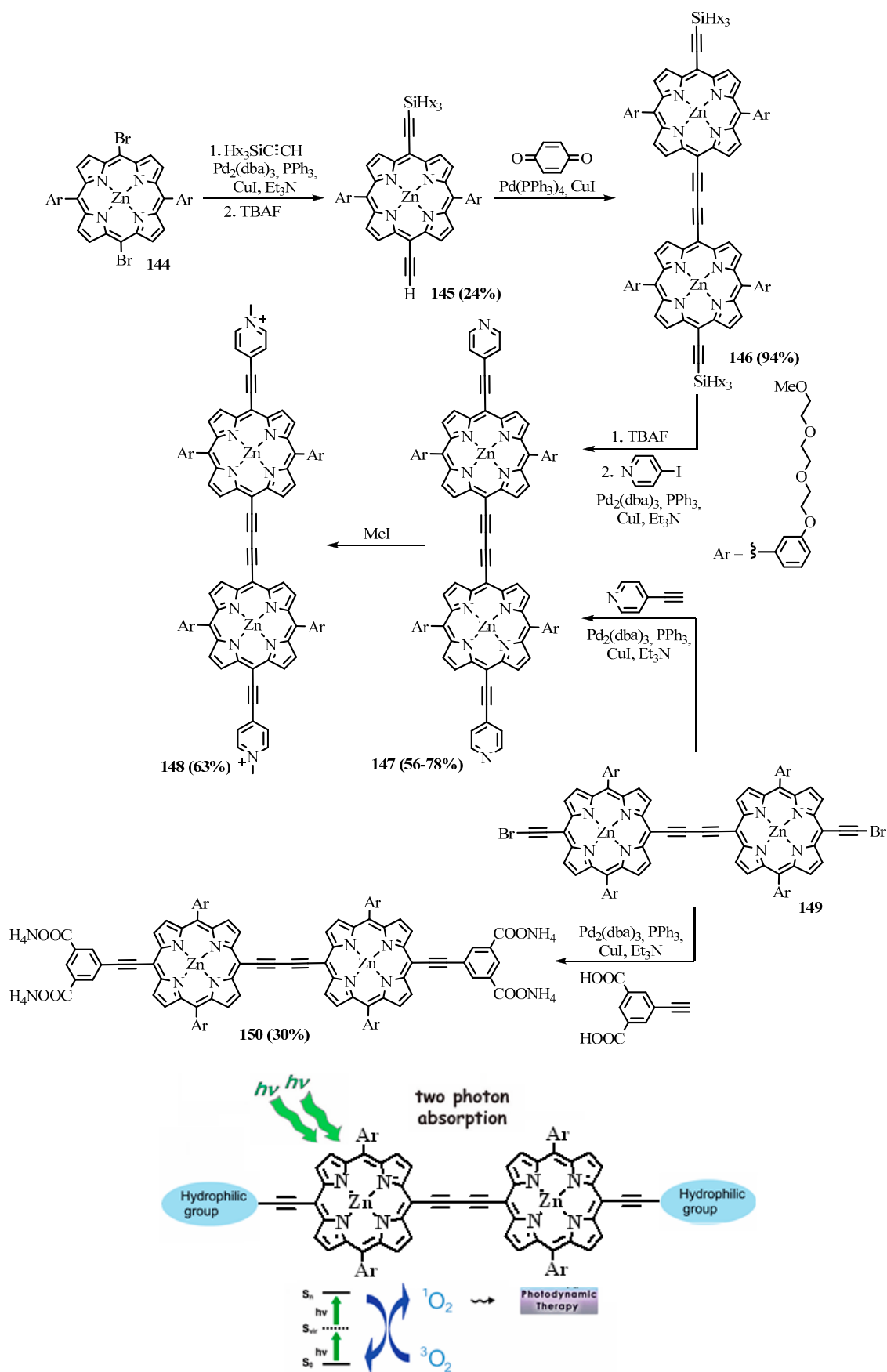
Further transformations of the acetylenylporphyrins include oxidative coupling, 1,3-dipolar cycloaddition, and nucleophilic addition. Glaser oxidative coupling of *meso*-acetylenylporphyrins was used to obtain porphyrin dimers as well as conjugates with other acetylenyl substituted compounds, but the yields of the oxidative cross-coupling are generally low due to the homocouplings. For example, 5,15-bisacetylenylporphyrin **141** was coupled with an excess of *meso*-acetylenyl-OEP, leading to the porphyrin triad **142** linked by butadiyne bridges with a 25% yield, along with a larger amount of the OEP dimer **143** formed by homocoupling (Scheme 56) [95]. The conjugation in the triad led to the splitting of the Soret band of OEP into two main bands with clear maxima at 429 and 481 nm and a bathochromic shift of the Q band to 670 nm. Furthermore, a dramatic bathochromic shift of the Q-band by 70 nm was observed in pyridine compared to that in chloroform, probably due to the coordination of the pyridine molecule as an axial ligand onto the Ni cation, though Ni porphyrinates do not usually coordinate extra ligands.



**Scheme 56.** Synthesis of porphyrin dimer and trimer with butadiyne bridge using Glaser oxidative coupling.

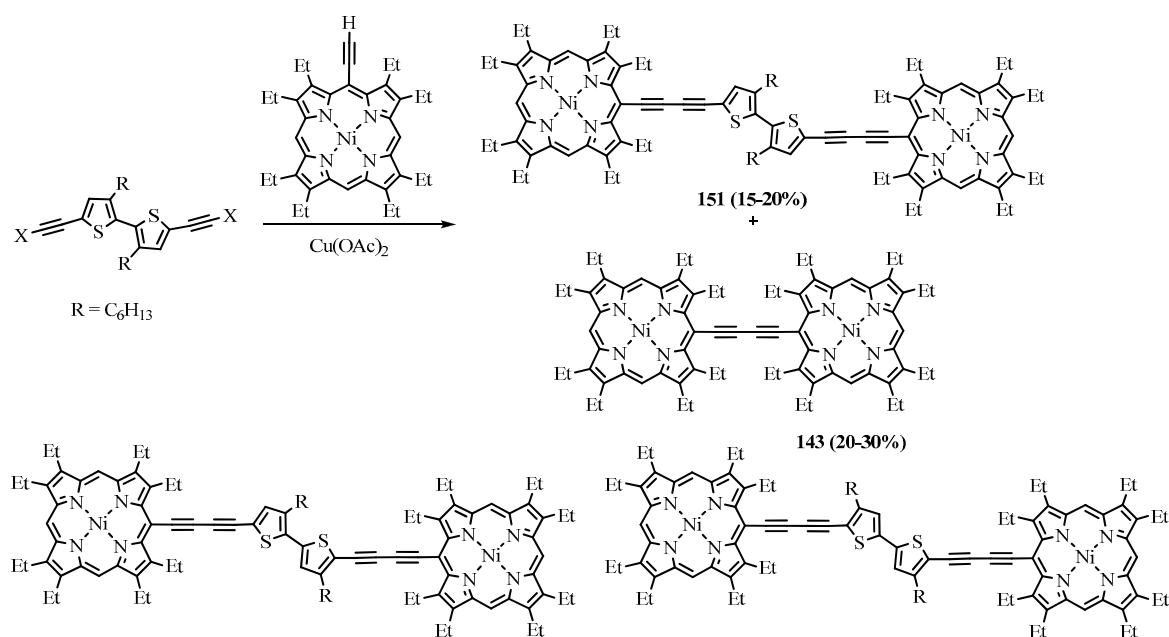
The butadiyne-linked *meso*-diarylporphyrin dimer **148** functionalized with hydrophilic groups was obtained using a sequence of Sonogashira and Glaser-type oxidative coupling reactions. First, *meso*-di(trihexylsilylacetylenyl)-diarylporphyrin was obtained from easily accessible *meso*-dibromodiarylporphyrin **144** and trihexylsilylacetylene using the classical Sonogashira reaction. The partial deprotection of the triple bond with TBAF proceeded with a low 29% yield. The half-protected bisacetylenylporphyrin **145** was dimerized using oxidative coupling in modified conditions catalyzed by Pd(PPh<sub>3</sub>)<sub>4</sub>, CuI, and 1,4-benzoquinone as an oxidant. These conditions provided a high 94% yield of dimer **146** bridged by butadiyne linkers. The presence of two *meso*-trihexylsilylacetylenyl groups in the dimer allowed for further functionalization using Sonogashira coupling with iodo-substituted hydrophilic fragments (Scheme 57) [116]. The obtained dyes possess red-shifted absorption bands in a region of 700–800 nm and a high two-photon absorption cross-section. These properties are important for application in PDT, and the porphyrin dimer dyes were studied as photosensitizers and were found to be more effective than the commercial drug Visudyne<sup>®</sup> in two-photon PDT [40].





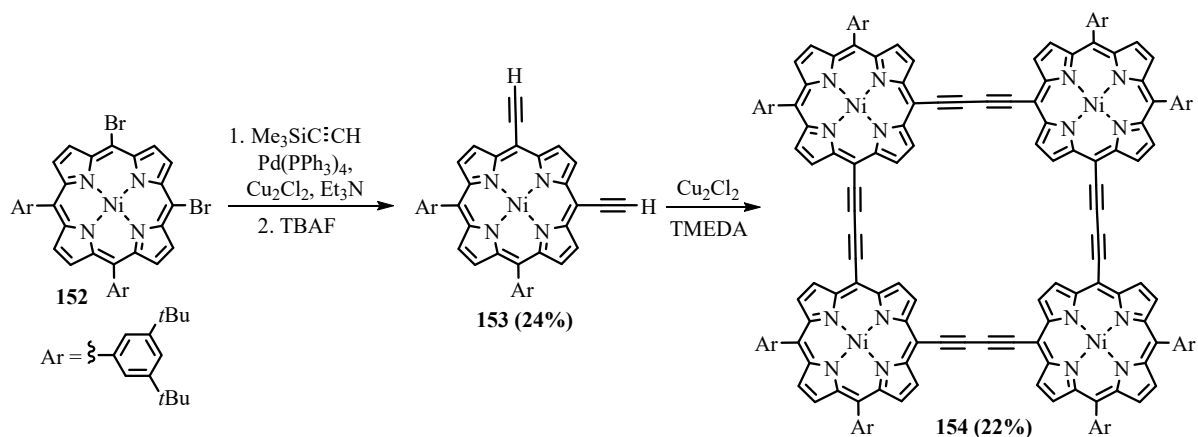
Scheme 57. Synthesis of methylpyridinium dimer 3 and carboxylate dimer 6 via Sonogashira coupling.

A series of bisporphyrins linked by bithiophene and butadiyne groups were obtained using oxidative cross-coupling of *meso*-acetylenyl-OEP with bisacetylenylbithiophene and oligomeric bithiophenes [97]. The coupling was carried out in the presence of copper(II) acetate in a mixture of pyridine and methanol. Yields of cross-coupled products were 15–20%, together with 20–30% yields of the diacetylene-bridged OEP dimer (Scheme 58). The position of the hexyl substituents in bithiophene determines the relative orientation of thiophene rings, which plays an important role in electronic communications between the two terminal OEP rings.



**Scheme 58.** Synthesis of bisporphyrins linked by bithiophene and butadiyne linkers using oxidative coupling.

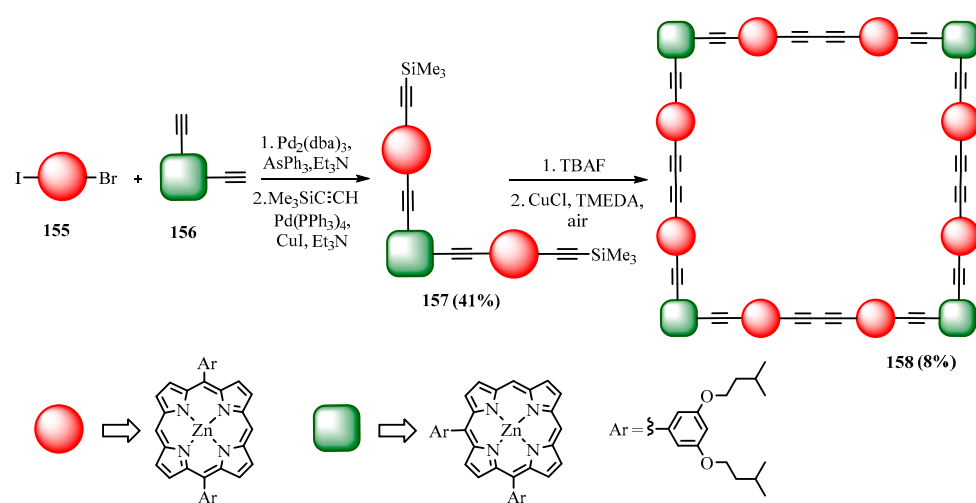
A series of *meso*-diarylporphyrin dimers linked by oligoacetylenes were obtained using Glaser coupling of *meso*-(oligoethynyl)porphyrins [94]. The similar coupling of the 5,10-diethynyl-15,20-diarylporphyrin **153** led to the formation of the square-shaped porphyrin tetramer **154** (Scheme 59) [117]. The positions of both the Soret (503) and Q (659 nm) bands were bathochromically shifted by about  $2900\text{ cm}^{-1}$  relative to the monomer but remained similar to those of the corresponding linear tetramer [118].



**Scheme 59.** Synthesis of the square porphyrin tetramer.

A square cyclic porphyrin dodecamer **158** with ethynyl linkers was obtained via the tetramerization of a T-shaped trimer **157** using Glaser oxidation coupling [119]. The synthe-

sis of the trimer was based on the Sonogashira reaction of 5,10-diethynyl-15,20-porphyrin **156** with 5-iodo-15-bromo-10,20-diarylporphyrin **157** (Scheme 60). The molecule was easily visualized using STM. The round-shaped octamer with butadiyne linkers **161** was synthesized via oxidative coupling of the 5,15-diethynyl-10,20-diarylporphyrin **159** using a template with palladium/copper catalysts and iodine as an oxidant to give the cyclooctamer **161** with a 14% yield (Scheme 61) [120]. A similar cyclohexamer was obtained with a smaller template by oxidizing trimerization of the corresponding dimer [121]. Absorption and emission spectra showed that  $\pi$ -conjugation and interchromophore communication in the nanoring are stronger than in its linear analog and angled square-shaped macrocycles. The giant porphyrin cyclooligomers can be applied as artificial light-harvesting antennas. The similarity between these nanorings and the natural chlorophyll-based LH2 light-harvesting system [122] allows us to model the photosynthetic center with these artificial molecules [123]. Middle-sized, angled cycles like square porphyrin tetramer and dodecamer are host compounds that can coordinate suitable guest molecules, including fullerenes.



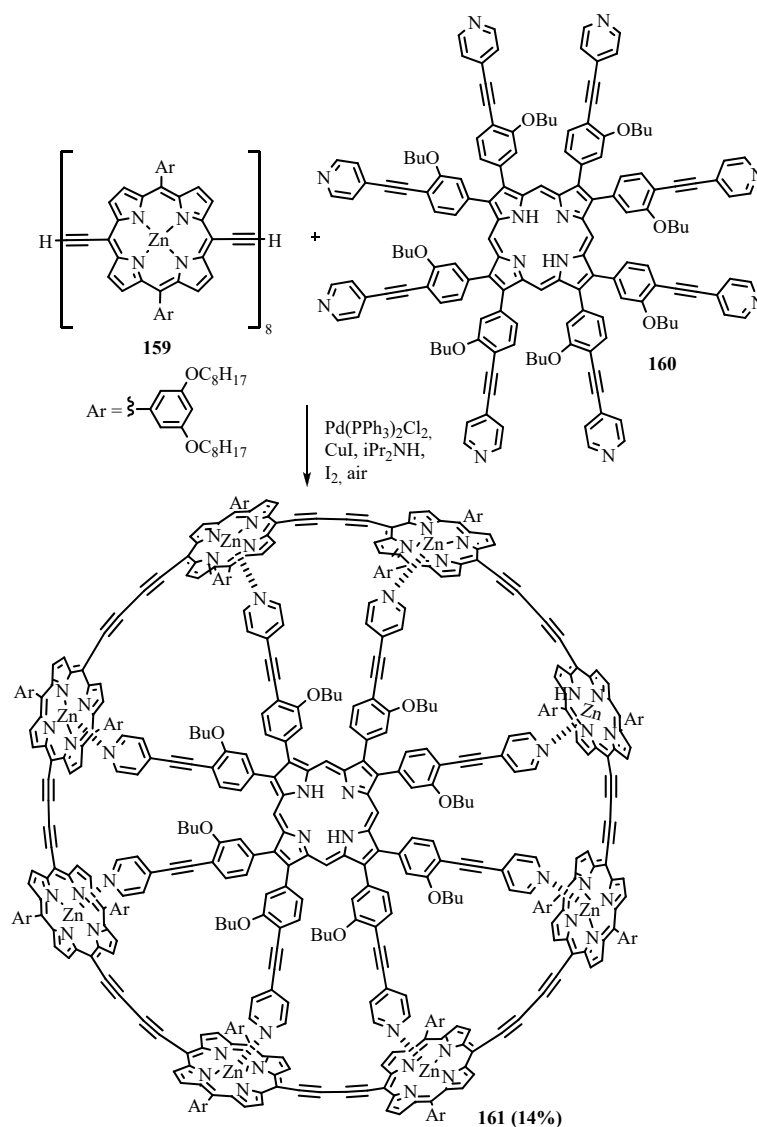
**Scheme 60.** Synthesis of square porphyrin dodecamer.

Most of the porphyrin dimers, trimers, and oligomers, linked by carbon-carbon triple bonds, were synthesized using either Glaser type oxidative coupling or Sonogashira coupling reactions. The considerable bathochromic shifts of the absorption and emission bands were observed for all multiporphyrin compounds compared to the precursor monomers. The Qy absorption bands of the porphyrin dimers are even longer in wavelength than those of the chlorin monomers, reaching up to 720 nm, making them promising photosensitizers for PDT and other optical applications such as optical sensors, NLO materials, etc. [124,125].

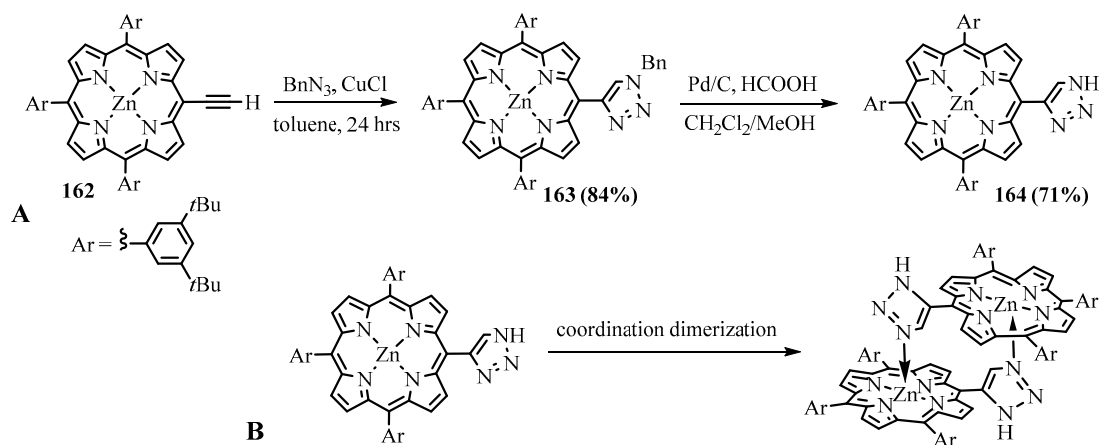
A copper-catalyzed 1,3-dipolar cycloaddition of azides to alkynes, called the “click” reaction, was used to create *meso*-1,2,3-triazole substituted porphyrin (Scheme 62A). The porphyrin self-assembles to form a slipped cofacial dimer **164** by the coordination of the triazole nitrogen atom to the zinc center of a second porphyrin moiety (Scheme 62B) [126].

The triazole group was also applied as a linker between porphyrin rings. Odobel obtained directly *meso-meso* triazole bridged dyads by the click reaction of Ni(II) and Zn(II) complexes of *meso*-ethynyltriarylporphyrin **166** with Ni(II) *meso*-azidotriarylporphyrin **165** (Scheme 63) [127]. Both Ni-Ni and Ni-Zn dyads were obtained, but the yield of the heterometallic dyad **167Zn** was notably lower (18%) compared to the yield of the Ni-Ni dyad **167Ni** (41%). The reaction proceeded for quite a long time (50 h) in DMF with copper sulfate as a catalyst and ascorbic acid. Asymmetrical  $\beta$ -*meso*-triazole-linked dyad **169** was synthesized from nickel complexes of 5-ethynyl-10,20-diphenylporphyrin **132Ni** and  $\beta$ -azido-*meso*-tetraphenylporphyrin **168** [128]. The reaction was carried out in the same conditions but proceeded much faster, being completed for 1.5 h with a high 98% yield (Scheme 63). It should be noted that in the case of the opposite reagent couple, namely

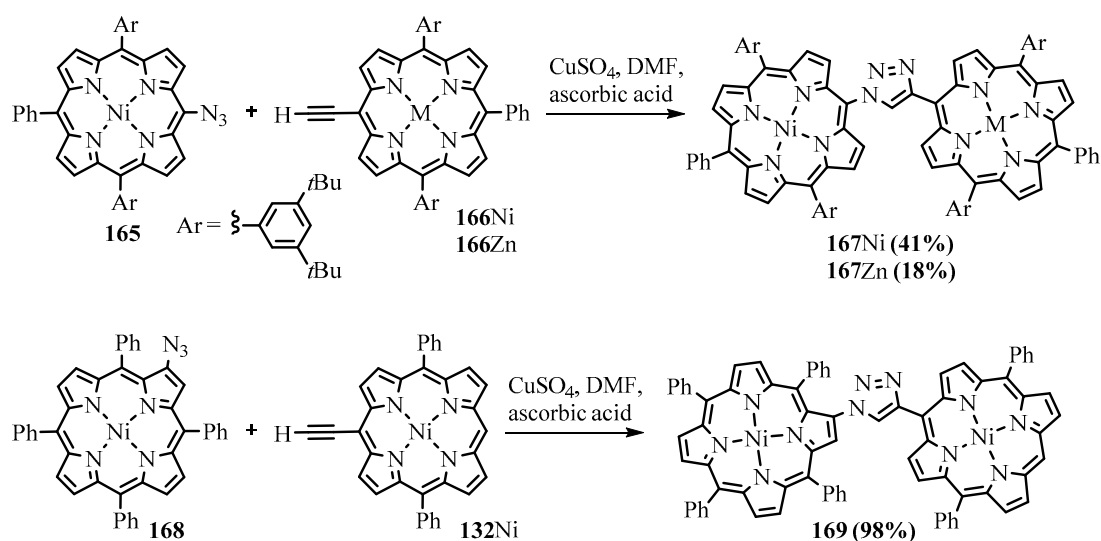
5-azido-10,20-diphenylporphyrin and  $\beta$ -ethynyl-*meso*-tetraphenylporphyrin, no reaction occurred under similar conditions.



**Scheme 61.** Template synthesis porphyrin cyclooctamer.

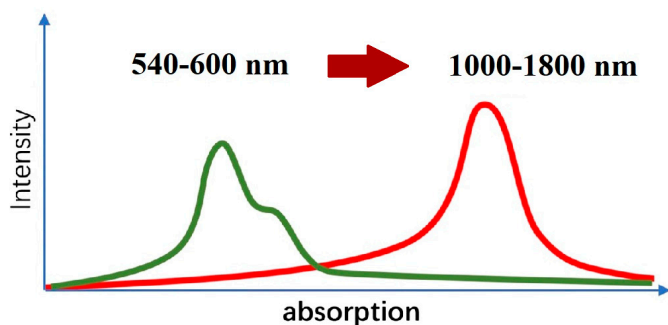
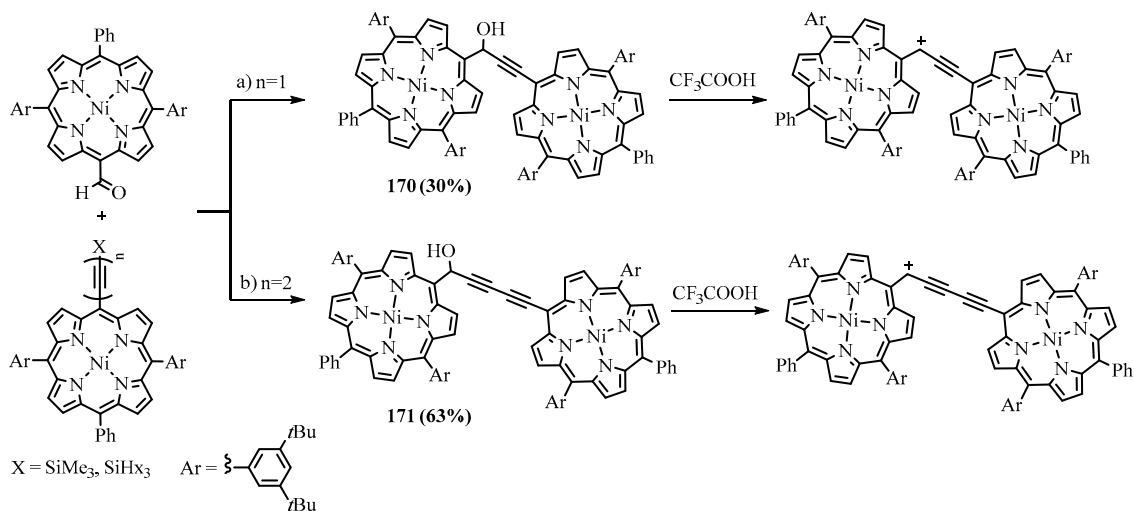


**Scheme 62.** (A) Synthesis of *meso*-1,2,3-triazole substituted porphyrin; (B) self-assembling to form a slipped cofacial dimer.



**Scheme 63.** Synthesis of 1,2,3-triazole-bridged porphyrin dyads.

The nucleophilic addition of alkynyl porphyrins to carbonyl compounds was used to prepare a series of porphyrin-dimer tertiary alcohols. Treatment of these alcohols with acid gave conjugated carbocations with three to nine carbon atoms bridging between the porphyrins (Scheme 64). All these carbocations show strong absorption in the near-IR region between 1000 and 1800 nm [129].



**Scheme 64.** Synthesis of bisporphyrins linked by bithiophene and butadiyne linkers using oxidative coupling.

## 5. Conclusions

Formyl, vinyl, and ethynyl are simple substituents that can easily be inserted into a tetrapyrrole macrocycle, providing suitable building blocks for the construction of porphyrin materials. The substitution at the *meso* position significantly affects the electron and optical properties of the porphyrins, and for this reason, it was the *meso*-derivatives that were considered. The reviewed works showed the rich potential of these synthons, opening the way to a variety of novel dyes with considerably modified properties that can be tuned by a choice of specific transformations of the starting building blocks. The products of such transformations are dyes for solar cells, light-harvesting antennas, photosensitizers for PDT, optical sensors, components for supramolecular ensembles, porous materials for storage and catalysis, etc. Particularly valuable are the biomedical applications of the tetrapyrrolic derivatives.

**Author Contributions:** V.S.T., A.O.S., O.I.K. and I.A.Z. have contributed equally. All authors have read and agreed to the published version of the manuscript.

**Funding:** This work was funded by the Russian Science Foundation, grant number 22-23-00903.

**Institutional Review Board Statement:** Not applicable.

**Informed Consent Statement:** Not applicable.

**Data Availability Statement:** Not applicable.

**Conflicts of Interest:** The authors declare no conflict of interest.

## Abbreviations

CuOEP	Cu(II) $\beta$ -octaethylporphyrin
DDQ	2,3-dichloro-5,6-dicyano-1,4-benzoquinone
DNA	deoxyribonucleic acid
DPP	5,15-diphenylporphyrin
DPP-CHO	5-formyl-10,20-diphenylporphyrin
DSSC	dye sensitized solar cells
MOF	metal-organic frameworks
NBS	<i>N</i> -bromosuccinimide
NiOEP	Ni(II) $\beta$ -octaethylporphyrin
NLO	nonlinear optical
OEC	$\beta$ -octaethylchlorin
OEP	$\beta$ -octaethylporphyrin
OEP-CHO	5-formyl- $\beta$ -octaethylporphyrin
PPPa	methyl pyropheophorbide- <i>a</i>
PPPd	methyl pyropheophorbide- <i>d</i>
PtOEP	Pt(II) $\beta$ -octaethylporphyrin
STM	scanning tunneling microscope
TMEDA	<i>N,N,N,N</i> -tetramethylethylenediamine
TPP	5,10,15,20-tetraphenylporphyrin
TrPP	5,10,15-triphenylporphyrin
ZnOEP	Zn(II) $\beta$ -octaethylporphyrin

## References

1. Koifman, O.I.; Ageeva, T.A. Main Strategies for the Synthesis of *meso*-Arylporphyrins. *Russ. J. Org. Chem.* **2022**, *58*, 443–479. [[CrossRef](#)]
2. Tyurin, V.S.; Uglov, A.; Beletskaya, I.P.; Stern, C.; Guillard, R. Survey of Synthetic Routes for Synthesis and Substitution in Porphyrins. In *Handbook of Porphyrin Science*; Kadish, K.M., Smith, K.M., Guillard, R., Eds.; World Scientific: Singapore, 2012; Volume 23, pp. 81–279.
3. Vicente, M.D.G.H.; Smith, K.M. Syntheses and Functionalizations of Porphyrin Macrocycles. *Curr. Org. Synth.* **2014**, *11*, 3–28. [[CrossRef](#)] [[PubMed](#)]
4. Senge, M.O. Stirring the porphyrin alphabet soup—Functionalization reactions for porphyrins. *Chem. Commun.* **2011**, *47*, 1943–1960. [[CrossRef](#)] [[PubMed](#)]

5. Ponomarev, G.V. Formylporphyrins and their derivatives in the chemistry of porphyrins (review). *Chem. Heterocycl. Compd.* **1994**, *30*, 1444–1465. [[CrossRef](#)]
6. Paolesse, R.; Nardis, S.; Monti, D.; Stefanelli, M.; Di Natale, C. Porphyrinoids for Chemical Sensor Applications. *Chem. Rev.* **2017**, *117*, 2517–2583. [[CrossRef](#)]
7. Nyman, E.S.; Hynninen, P.H. Research advances in the use of tetrapyrrolic photosensitizers for photodynamic therapy. *J. Photochem. Photobiol. B Biol.* **2004**, *73*, 1–28. [[CrossRef](#)]
8. Sternberg, E.D.; Dolphin, D.; Brückner, C. Porphyrin-based photosensitizers for use in photodynamic therapy. *Tetrahedron* **1998**, *54*, 4151–4202. [[CrossRef](#)]
9. Ethirajan, M.; Chen, Y.; Joshi, P.; Pandey, R.K. The role of porphyrin chemistry in tumor imaging and photodynamic therapy. *Chem. Soc. Rev.* **2011**, *40*, 340–362. [[CrossRef](#)]
10. Cerqueira, A.F.R.; Moura, N.M.M.; Serra, V.V.; Faustino, M.A.F.; Tomé, A.C.; Cavaleiro, J.A.S.; Neves, M.G.P.M.S.  $\beta$ -Formyl- and  $\beta$ -Vinylporphyrins: Magic Building Blocks for Novel Porphyrin Derivatives. *Molecules* **2017**, *22*, 1269. [[CrossRef](#)]
11. Mathew, S.; Yella, A.; Gao, P.; Humphry-Baker, R.; Curchod, B.F.E.; Ashari-Astani, N.; Tavernelli, I.; Rothlisberger, U.; Nazeeruddin, M.K.; Graetzel, M. Dye-sensitized solar cells with 13% efficiency achieved through the molecular engineering of porphyrin sensitizers. *Nat. Chem.* **2014**, *6*, 242–247. [[CrossRef](#)]
12. Burrell, A.K.; Officer, D.L. Functionalizing Porphyrins via Wittig Reactions: A Building Block Approach. *Synlett* **1998**, *1998*, 1297–1307. [[CrossRef](#)]
13. Ando, A.; Yamazaki, M.; Komura, M.; Sano, Y.; Hattori, N.; Omote, M.; Kumadaki, I. An efficient route to formyldeuteroporphyrins and their Wittig reaction. *Heterocycles* **1999**, *50*, 913–918. [[CrossRef](#)]
14. Dahms, K.; Senge, M.O.; Bakri Bakar, M. Exploration of meso-substituted formyl porphyrins and their Grignard and Wittig reactions. *Eur. J. Org. Chem.* **2007**, *2007*, 3833–3848. [[CrossRef](#)]
15. Runge, S.; Senge, M.O. Reaction of  $\beta$ -formylporphyrins with organometallic reagents—A facile method for the preparation of porphyrins with exocyclic double bonds. *Tetrahedron* **1999**, *55*, 10375–10390. [[CrossRef](#)]
16. Arnold, D.P.; Johnson, A.W.; Mahendran, M. Some reactions of meso-formyloctaethylporphyrin. *J. Chem. Soc. Perkin Trans. 1* **1978**, 366–370. [[CrossRef](#)]
17. Smith, K.M. The McMurry Reaction in Porphyrinoid Chemistry. In *Synthesis and Modifications of Porphyrinoids*; Paolesse, R., Ed.; Springer: Berlin/Heidelberg, Germany, 2014; pp. 1–34. [[CrossRef](#)]
18. Tkachenko, N.V.; Lemmetyinen, H.; Sonoda, J.; Ohkubo, K.; Sato, T.; Imahori, H.; Fukuzumi, S. Ultrafast Photodynamics of Exciplex Formation and Photoinduced Electron Transfer in Porphyrin–Fullerene Dyads Linked at Close Proximity. *J. Phys. Chem. A* **2003**, *107*, 8834–8844. [[CrossRef](#)]
19. Fuhrhop, J.-H.; Witte, L.; Sheldrick, W.S. Darstellung, Struktur und Reaktivität hochsubstituierter Porphyrine. *Justus Liebigs Ann. Der Chem.* **1976**, *1976*, 1537–1559. [[CrossRef](#)]
20. Ponomarev, G.V. Synthesis and properties of Schiff bases of mesoformylporphyrins (Review). *Chem. Heterocycl. Compd.* **1996**, *32*, 1263–1280. [[CrossRef](#)]
21. Hong, S.-K.; Jeoung, E.; Lee, C.-H. Meso-meso linked hybrid porphyrin arrays from meso-formylated porphyrins. *J. Porphyr. Phthalocyanines* **2005**, *9*, 285–289. [[CrossRef](#)]
22. Balakumar, A.; Muthukumar, K.; Lindsey, J.S. A New Route to meso-Formyl Porphyrins. *J. Org. Chem.* **2004**, *69*, 5112–5115. [[CrossRef](#)]
23. Senge, M.O.; Hatscher, S.S.; Wiehe, A.; Dahms, K.; Kelling, A. The Dithianyl Group as a Synthone in Porphyrin Chemistry: Condensation Reactions and Preparation of Formylporphyrins under Basic Conditions. *J. Am. Chem. Soc.* **2004**, *126*, 13634–13635. [[CrossRef](#)]
24. Seebach, D.; Corey, E.J. Generation and synthetic applications of 2-lithio-1,3-dithianes. *J. Org. Chem.* **1975**, *40*, 231–237. [[CrossRef](#)]
25. Takanami, T.; Wakita, A.; Sawaizumi, A.; Iso, K.; Onodera, H.; Suda, K. One-Pot Synthesis of meso-Formylporphyrins by SNAr Reaction of 5,15-Disubstituted Porphyrins with (2-Pyridyldimethylsilyl)methylolithium. *Org. Lett.* **2008**, *10*, 685–687. [[CrossRef](#)] [[PubMed](#)]
26. Takanami, T.; Wakita, A.; Matsumoto, J.; Sekine, S.; Suda, K. An efficient one-pot procedure for asymmetric bifunctionalization of 5,15-disubstituted porphyrins: A simple preparation of meso-acyl-, alkoxy-carbonyl-, and carbamoyl-substituted meso-formylporphyrins. *Chem. Commun.* **2009**, 101–103. [[CrossRef](#)]
27. Takanami, T.; Matsumoto, J.; Kumagai, Y.; Sawaizumi, A.; Suda, K. A facile one-pot preparation of meso-hydroxymethylporphyrins via a sequential SNAr reaction with (2-pyridyldimethylsilyl)methylolithium followed by hydrolysis and aerobic oxidation. *Tetrahedron Lett.* **2009**, *50*, 68–70. [[CrossRef](#)]
28. Takanami, T.; Hayashi, S.; Iso, K.; Matsumoto, J.; Hino, F. An efficient one-pot protocol for asymmetric bifunctionalization of 5,15-disubstituted porphyrins: Direct access to meso-activated alkenyl-substituted meso-formylporphyrins. *Tetrahedron Lett.* **2011**, *52*, 5345–5348. [[CrossRef](#)]
29. Fujimoto, K.; Yorimitsu, H.; Osuka, A. Efficient Synthesis and Versatile Reactivity of Porphyrinyl Grignard Reagents. *Eur. J. Org. Chem.* **2014**, *2014*, 4327–4334. [[CrossRef](#)]
30. Inhoffen, H.H.; Fuhrhop, J.-H.; Voigt, H.; Brockmann, H., Jr. Zur weiteren Kenntnis des Chlorophylls und des Hämins, VI. Formylierung der meso-Kohlenstoffatome von Alkyl-substituierten Porphyrinen. *Justus Liebigs Ann. Der Chem.* **1966**, *695*, 133–143. [[CrossRef](#)]



31. Johnson, A.W.; Oldfield, D. meso-Substitution products of  $\alpha$ etioporphyrin I. *J. Chem. Soc. C Org.* **1966**, 794–798. [[CrossRef](#)]
32. Ponomarev, G.V.; Rozynov, B.V. Synthesis of copper and iron complexes of meso-substituted etioporphyrin derivatives. *Chem. Heterocycl. Compd.* **1973**, *9*, 1065–1068. [[CrossRef](#)]
33. Volov, A.N.; Zamilatskov, I.A.; Mikhel, I.S.; Erzina, D.R.; Ponomarev, G.V.; Koifman, O.I.; Tsivadze, A.Y. Synthesis of the First Azomethine Derivatives of Pd-II Coproporphyrins I and II. *Macroheterocycles* **2014**, *7*, 256–261. [[CrossRef](#)]
34. Tyurin, V.S.; Erzina, D.R.; Zamilatskov, I.A.; Chernyadyev, A.Y.; Ponomarev, G.V.; Yashunskiy, D.V.; Maksimova, A.V.; Krasnovskiy, A.A.; Tsivadze, A.Y. Palladium Complexes of Azomethine Derivatives of Porphyrins as Potential Photosensitizers. *Macroheterocycles* **2015**, *8*, 376–383. [[CrossRef](#)]
35. Erzina, D.R.; Zamilatskov, I.A.; Stanetskaya, N.M.; Tyurin, V.S.; Kozhemyakin, G.L.; Ponomarev, G.V.; Chernyshev, V.V.; Fitch, A.N. Transformations of meso-Iminofunctionalized Pd(II) and Ni(II)-Complexes of  $\beta$ -Alkylsubstituted Porphyrins. *Eur. J. Org. Chem.* **2019**, *2019*, 1508–1522. [[CrossRef](#)]
36. Papkovsky, D.B.; Ponomarev, G.V.; Wolfbeis, O.S. Protonation of porphyrins in liquid PVC membranes: Effects of anionic additives and application to pH-sensing. *J. Photochem. Photobiol. A Chem.* **1997**, *104*, 151–158. [[CrossRef](#)]
37. Borchert, N.B.; Ponomarev, G.V.; Kerry, J.P.; Papkovsky, D.B. O<sub>2</sub>/pH Multisensor Based on One Phosphorescent Dye. *Anal. Chem.* **2011**, *83*, 18–22. [[CrossRef](#)] [[PubMed](#)]
38. Zhdanov, A.V.; Li, L.; Yang, P.; Shkirdova, A.O.; Tang, S.; Yashunsky, D.V.; Ponomarev, G.V.; Zamilatskov, I.A.; Papkovsky, D.B. Advanced multi-modal, multi-analyte optochemical sensing platform for cell analysis. *Sens. Actuators B Chem.* **2022**, *355*, 131116. [[CrossRef](#)]
39. Harper, S.R.; Pfrunder, M.C.; Esdaile, L.J.; Jensen, P.; McMurtrie, J.C.; Arnold, D.P. Synthetic, Structural, and Spectroscopic Studies of Bis(porphyrin)zinc Complexes Linked by Two-Atom Conjugating Bridges. *Eur. J. Org. Chem.* **2015**, *2015*, 2807–2825. [[CrossRef](#)]
40. Dahlstedt, E.; Collins, H.A.; Balaz, M.; Kuimova, M.K.; Khurana, M.; Wilson, B.C.; Phillips, D.; Anderson, H.L. One- and two-photon activated phototoxicity of conjugated porphyrin dimers with high two-photon absorption cross sections. *Org. Biomol. Chem.* **2009**, *7*, 897–904. [[CrossRef](#)]
41. Yashunsky, D.V.; Morozova, Y.V.; Ponomarev, G.V. Chemistry of meso-formylporphyrin oximes. An elegant synthesis of meso-cyanoporphyrins. *Chem. Heterocycl. Compd.* **2000**, *36*, 485–486. [[CrossRef](#)]
42. Yashunsky, D.V.; Morozova, Y.V.; Ponomarev, G.V. Chemistry of meso-formylporphyrin oximes. The synthesis of the hetero analog of australochlorin. *Chem. Heterocycl. Compd.* **2000**, *36*, 487–488. [[CrossRef](#)]
43. Yashunsky, D.V.; Morozova, Y.V.; Ponomarev, G.V. Chemistry of Metal Complexes of Oximes of meso-Formylporphyrins. Oxidative Cyclization to Metal Complexes of Hydroxy-1,2-oxazinochlorins. *Chem. Heterocycl. Compd.* **2001**, *37*, 380–381. [[CrossRef](#)]
44. Ponomarev, G.V.; Shul'ga, A.M. Porphyrins. 16. Thermolysis of schiff bases of meso-formylporphyrins—A convenient method for the synthesis of porphyrins with a cyclopentane ring. *Chem. Heterocycl. Compd.* **1984**, *20*, 383–388. [[CrossRef](#)]
45. Ponomarev, G.V.; Shul'ga, A.M. Porphyrins. 22. Synthesis of porphyrins with two cyclopentane rings. *Chem. Heterocycl. Compd.* **1987**, *23*, 757–762. [[CrossRef](#)]
46. Ponomarev, G.V.; Shul'ga, A.M.; Rozynov, B.V. Porphyrin. *Chem. Heterocycl. Compd.* **1993**, *29*, 155–162. [[CrossRef](#)]
47. Shkirdova, A.O.; Zamilatskov, I.A.; Stanetskaya, N.M.; Tafeenko, V.A.; Tyurin, V.S.; Chernyshev, V.V.; Ponomarev, G.V.; Tsivadze, A.Y. Synthesis and Study of New N-Substituted Hydrazones of Ni(II) Complexes of beta-Octaethylporphyrin and Coproporphyrin I Tetraethyl Ester. *Macroheterocycles* **2017**, *10*, 480–486. [[CrossRef](#)]
48. Kozhemyakin, G.L.; Tyurin, V.S.; Shkirdova, A.O.; Belyaev, E.S.; Kirinova, E.S.; Ponomarev, G.V.; Chistov, A.A.; Aralov, A.V.; Tafeenko, V.A.; Zamilatskov, I.A. Carbene functionalization of porphyrinoids through tosylhydrazones. *Org. Biomol. Chem.* **2021**, *19*, 9199–9210. [[CrossRef](#)] [[PubMed](#)]
49. Belyaev, E.S.; Shkirdova, A.O.; Kozhemyakin, G.L.; Tyurin, V.S.; Emets, V.V.; Grinberg, V.A.; Cheshkov, D.A.; Ponomarev, G.V.; Tafeenko, V.A.; Radchenko, A.S.; et al. Azines of porphyrinoids. Does azine provide conjugation between chromophores? *Dye Pigment.* **2021**, *191*, 109354. [[CrossRef](#)]
50. Andreeva, V.D.; Ponomarev, G.V.; Shkirdova, A.O.; Tyurin, V.S.; Zamilatskova, I.A. Modification of  $\beta$ -Octaethylporphyrin via Insertion of Amino and Azino Groups into meso-Positions. *Macroheterocycles* **2021**, *14*, 201–207. [[CrossRef](#)]
51. Birin, K.P.; Gorbunova, Y.G.; Tsivadze, A.Y. New approach for post-functionalization of meso-formylporphyrins. *RSC Adv.* **2015**, *5*, 67242–67246. [[CrossRef](#)]
52. Jiang, J.; Liu, D.; Zhao, Y.; Wu, F.; Yang, K.; Wang, K. Synthesis, DNA binding mode, singlet oxygen photogeneration and DNA photocleavage activity of ruthenium compounds with porphyrin-imidazo[4,5-f]phenanthroline conjugated ligand. *Appl. Organomet. Chem.* **2018**, *32*, e4468. [[CrossRef](#)]
53. Smith, M.J.; Blake, I.M.; Clegg, W.; Anderson, H.L. Push–pull quinoidal porphyrins. *Org. Biomol. Chem.* **2018**, *16*, 3648–3654. [[CrossRef](#)] [[PubMed](#)]
54. Chen, C.; Zhu, Y.-Z.; Fan, Q.-J.; Song, H.-B.; Zheng, J.-Y. Syntheses, Crystal Structure, and Spectroscopic Properties of Meso–Meso-Linked Porphyrin–Corrole Hybrids. *Chem. Lett.* **2013**, *42*, 936–938. [[CrossRef](#)]
55. Murugavel, M.; Reddy, R.V.R.; Sankar, J. A new meso–meso directly-linked corrole–porphyrin–corrole hybrid: Synthesis and photophysical properties. *RSC Adv.* **2014**, *4*, 13669–13672. [[CrossRef](#)]
56. Higashino, T.; Imahori, H. Development of Efficient Sensitizers Based on Porphyrin Dimers and Fused Porphyrins for Dye-Sensitized Solar Cells. *ECS Meet. Abstr.* **2021**, *MA2021-01*, 769. [[CrossRef](#)]

57. Ponomarev, G.V.; Sidorov, A.N. Porphyrins. *Chem. Heterocycl. Compd.* **1977**, *13*, 742–747. [[CrossRef](#)]
58. Jiang, X.; Nurco, D.J.; Smith, K.M. Direct meso-alkylation of meso-formylporphyrins using Grignard reagents. *Chem. Commun.* **1996**, 1759–1760. [[CrossRef](#)]
59. Locos, O.B.; Arnold, D.P. The Heck reaction for porphyrin functionalisation: Synthesis of meso-alkenyl monoporphyrins and palladium-catalysed formation of unprecedented meso- $\beta$  ethene-linked diporphyrins. *Org. Biomol. Chem.* **2006**, *004*, 902–916. [[CrossRef](#)]
60. van der Haas, R.N.S.; de Jong, R.L.P.; Noushazar, M.; Erkelens, K.; Smijs, T.G.M.; Liu, Y.; Gast, P.; Schuitmaker, H.J.; Lugtenburg, J. The Synthesis of the Dimethyl Ester of Quino[4,4a,5,6-efg]-Annulated 7-Demethyl-8-deethylmesoporphyrin and Three of Its Isomers with Unprecedented peri-Condensed Quinoline Porphyrin Structures. Molecules with Outstanding Properties as Sensitizers for Photodynamic Therapy in the Far-Red Region of the Visible Spectrum. *Eur. J. Org. Chem.* **2004**, *2004*, 4024–4038. [[CrossRef](#)]
61. Kessel, D.; Morgan, A. Photosensitization with Etiobenzochlorins and Octaethylbenzochlorins. *Photochem. Photobiol.* **1993**, *58*, 521–526. [[CrossRef](#)]
62. Morgan, A.R.; Rampersaud, A.; Garbo, G.M.; Keck, R.W.; Selman, S.H. New sensitizers for photodynamic therapy. Controlled synthesis of purpurins and their effect on normal tissue. *J. Med. Chem.* **1989**, *32*, 904–908. [[CrossRef](#)]
63. Li, G.; Graham, A.; Potter, W.; Grossman, Z.D.; Oseroff, A.; Dougherty, T.J.; Pandey, R.K. A Simple and Efficient Approach for the Synthesis of Fluorinated and Nonfluorinated Octaethylporphyrin-Based Benzochlorins with Variable Lipophilicity, Their in Vivo Tumor Uptake, and the Preliminary in Vitro Photosensitizing Efficacy. *J. Org. Chem.* **2001**, *66*, 1316–1325. [[CrossRef](#)] [[PubMed](#)]
64. Meunier, I.; Pandey, R.K.; Senge, M.O.; Dougherty, T.J.; Smith, K.M. Benzoporphyrin derivatives: Synthesis, structure and preliminary biological activity. *J. Chem. Soc. Perkin Trans. 1* **1994**, 961–969. [[CrossRef](#)]
65. Li, G.; Pandey, S.K.; Graham, A.; Dobhal, M.P.; Mehta, R.; Chen, Y.; Gryshuk, A.; Rittenhouse-Olson, K.; Oseroff, A.; Pandey, R.K. Functionalization of OEP-Based Benzochlorins To Develop Carbohydrate-Conjugated Photosensitizers. Attempt To Target  $\beta$ -Galactoside-Recognized Proteins. *J. Org. Chem.* **2004**, *69*, 158–172. [[CrossRef](#)] [[PubMed](#)]
66. Kohli, D.H.; Morgan, A.R. Preparation of substituted chlorins and benzochlorins. *Bioorg. Med. Chem. Lett.* **1995**, *5*, 2175–2178. [[CrossRef](#)]
67. Arnold, D.P.; Nitschinsk, L.J. Porphyrin Dimers Linked by Conjugated Butadiynes. *Tetrahedron* **1992**, *48*, 8781–8792. [[CrossRef](#)]
68. Arnold, D.P.; Hartnell, R.D. Butadiyne-linked bis(chlorin) and chlorin-porphyrin dyads and an improved synthesis of bis[octaethylporphyrinatonicel(II)-5-yl]butadiyne using the Takai iodoalkenation. *Tetrahedron* **2001**, *57*, 1335–1345. [[CrossRef](#)]
69. Vicente, M.G.H.; Smith, K.M. Vilsmeier reactions of porphyrins and chlorins with 3-(dimethylamino)acrolein to give meso-(2-formylvinyl)porphyrins: New syntheses of benzochlorins, benzoisobacteriochlorins, and benzobacteriochlorins and reductive coupling of porphyrins and chlorins using low-valent titanium complexes. *J. Org. Chem.* **1991**, *56*, 4407–4418. [[CrossRef](#)]
70. Rong, J.; Wu, Y.; Ji, X.; Zhao, T.; Yin, B.; Rao, Y.; Zhou, M.; Osuka, A.; Xu, L.; Song, J. Porphyrinatonicel(II)-Cyclopentene and Porphyrinatonicel(II)-Cyclopentadiene Hybrids: Zirconacyclopentadiene-Mediated Syntheses, Structures, and Mechanistic Study. *Org. Lett.* **2022**, *24*, 6128–6132. [[CrossRef](#)]
71. Wang, Q.; Ma, F.; Tang, W.; Zhao, S.; Li, C.; Xie, Y. A novel nitroethylene-based porphyrin as a NIR fluorescence turn-on probe for biothiols based on the Michael addition reaction. *Dye Pigm.* **2018**, *148*, 437–443. [[CrossRef](#)]
72. Muthiah, C.; Taniguchi, M.; Kim, H.-J.; Schmidt, I.; Kee, H.L.; Holten, D.; Bocian, D.F.; Lindsey, J.S. Synthesis and Photophysical Characterization of Porphyrin, Chlorin and Bacteriochlorin Molecules Bearing Tethers for Surface Attachment. *Photochem. Photobiol.* **2007**, *83*, 1513–1528. [[CrossRef](#)]
73. Chen, B.; Ding, Y.; Li, X.; Zhu, W.; Hill, J.P.; Ariga, K.; Xie, Y. Steric hindrance-enforced distortion as a general strategy for the design of fluorescence “turn-on” cyanide probes. *Chem. Commun.* **2013**, *49*, 10136–10138. [[CrossRef](#)] [[PubMed](#)]
74. Shkirdova, A.O.; Orlova, E.A.; Ponomarev, G.V.; Tyurin, V.S.; Zamilatskov, I.A.; Buryak, A.K. Synthesis of  $\beta$ -Octaethylporphyrin Conjugates with Nitrogen and Sulfur Containing Heterocycles. *Macrocyclics* **2021**, *14*, 208–212. [[CrossRef](#)]
75. DiMagno, S.G.; Lin, V.S.Y.; Therien, M.J. Facile elaboration of porphyrins via metal-mediated cross-coupling. *J. Org. Chem.* **1993**, *58*, 5983–5993. [[CrossRef](#)]
76. Kato, A.; Hartnell, R.D.; Yamashita, M.; Miyasaka, H.; Sugiura, K.-I.; Arnold, D.P. Selective meso-monobromination of 5,15-diarylporphyrins via organopalladium porphyrins. *J. Porphyr. Phthalocyanines* **2004**, *8*, 1222–1227. [[CrossRef](#)]
77. Shi, X.; Amin, S.R.; Liebeskind, L.S. 3-Cyclobutenyl-1,2-dione-Substituted Porphyrins. A General and Efficient Entry to Porphyrin–Quinone and Quinone–Porphyrin–Quinone Architectures. *J. Org. Chem.* **2000**, *65*, 1650–1664. [[CrossRef](#)]
78. Locos, O.; Bašić, B.; McMurtrie, J.C.; Jensen, P.; Arnold, D.P. Homo- and Heteronuclear meso,meso-(E)-Ethene-1,2-diyl-Linked Diporphyrins: Preparation, X-ray Crystal Structure, Electronic Absorption and Emission Spectra and Density Functional Theory Calculations. *Chem.—A Eur. J.* **2012**, *18*, 5574–5588. [[CrossRef](#)]
79. Arnold, D.P.; Gaete-Holmes, R.; Johnson, A.W.; Smith, A.R.P.; Williams, G.A. Wittig condensation products from nickel meso-formyl-octaethyl-porphyrin and -aetioporphyrin I and some cyclisation reactions. *J. Chem. Soc. Perkin Trans. 1* **1978**, 1660–1670. [[CrossRef](#)]
80. Glowacka-Sobotta, A.; Wrotynski, M.; Kryjewski, M.; Sobotta, L.; Mielcarek, J. Porphyrinoids in photodynamic diagnosis and therapy of oral diseases. *J. Porphyr. Phthalocyanines* **2019**, *23*, 1–10. [[CrossRef](#)]
81. Moreira, L.M.; Vieira dos Santos, F.; Lyon, J.P.; Maftoum-Costa, M.; Pacheco-Soares, C.; Soares da Silva, N. Photodynamic Therapy: Porphyrins and Phthalocyanines as Photosensitizers. *Aust. J. Chem.* **2008**, *61*, 741–754. [[CrossRef](#)]

82. Morgan, A.; Garbo, G.; Rampersaud, A.; Skalkos, D.; Keck, R.; Selman, S. *Photodynamic Action Of Benzochlorins*; SPIE: Bellingham, WA, USA, 1989; Volume 1065.
83. Frampton, M.J.; Akdas, H.; Cowley, A.R.; Rogers, J.E.; Slagle, J.E.; Fleitz, P.A.; Drobizhev, M.; Rebane, A.; Anderson, H.L. Synthesis, Crystal Structure, and Nonlinear Optical Behavior of  $\beta$ -Unsubstituted meso-meso E-Vinylene-Linked Porphyrin Dimers. *Org. Lett.* **2005**, *7*, 5365–5368. [[CrossRef](#)]
84. Tokuji, S.; Awane, H.; Yorimitsu, H.; Osuka, A. Direct Arylation of meso-Formyl Porphyrin. *Chem.—A Eur. J.* **2013**, *19*, 64–68. [[CrossRef](#)]
85. Belyaev, E.S.; Kozhemyakin, G.L.; Tyurin, V.S.; Frolova, V.V.; Lonin, I.S.; Ponomarev, G.V.; Buryak, A.K.; Zamilatskov, I.A. Direct C–H borylation of vinylporphyrins via copper catalysis. *Org. Biomol. Chem.* **2022**, *20*, 1926–1932. [[CrossRef](#)]
86. Orlova, E.A.; Romanenko, Y.V.; Tyurin, V.S.; Shkirdova, A.O.; Belyaev, E.S.; Grigoriev, M.S.; Koifman, O.I.; Zamilatskov, I.A. Dimer of Pd(II)  $\beta$ -octaethylporphyrin bound by a 1,3-butadiene bridge. *Macroheterocycles* **2022**, *15*, 139–146. [[CrossRef](#)]
87. Tanaka, T.; Osuka, A. Conjugated porphyrin arrays: Synthesis, properties and applications for functional materials. *Chem. Soc. Rev.* **2015**, *44*, 943–969. [[CrossRef](#)] [[PubMed](#)]
88. Chachisvilis, M.; Chirvony, V.S.; Shulga, A.M.; Källebring, B.; Larsson, S.; Sundström, V. Spectral and Photophysical Properties of Ethylene-Bridged Side-to-Side Porphyrin Dimers. 1. Ground-State Absorption and Fluorescence Study and Calculation of Electronic Structure of trans-1,2-Bis(meso-octaethylporphyrinyl)ethene. *J. Phys. Chem.* **1996**, *100*, 13857–13866. [[CrossRef](#)]
89. Screen, T.E.O.; Blake, I.M.; Rees, L.H.; Clegg, W.; Borwick, S.J.; Anderson, H.L. Making conjugated connections to porphyrins: A comparison of alkyne, alkene, imine and azo links. *J. Chem. Soc. Perkin Trans. 1* **2002**, 320–329. [[CrossRef](#)]
90. Rintoul, L.; Harper, S.R.; Arnold, D.P. A systematic theoretical study of the electronic structures of porphyrin dimers: DFT and TD-DFT calculations on diporphyrins linked by ethane, ethene, ethyne, imine, and azo bridges. *Phys. Chem. Chem. Phys.* **2013**, *15*, 18951–18964. [[CrossRef](#)]
91. Yang, S.I.; Lammi, R.K.; Seth, J.; Riggs, J.A.; Arai, T.; Kim, D.; Bocian, D.F.; Holten, D.; Lindsey, J.S. Excited-State Energy Transfer and Ground-State Hole/Electron Hopping in p-Phenylene-Linked Porphyrin Dimers. *J. Phys. Chem. B* **1998**, *102*, 9426–9436. [[CrossRef](#)]
92. Lin, V.S.-Y.; DiMagno, S.G.; Therien, M.J. Highly Conjugated, Acetylenyl Bridged Porphyrins: New Models for Light-Harvesting Antenna Systems. *Science* **1994**, *264*, 1105–1111. [[CrossRef](#)]
93. Taylor, P.N.; Anderson, H.L. Cooperative Self-Assembly of Double-Strand Conjugated Porphyrin Ladders. *J. Am. Chem. Soc.* **1999**, *121*, 11538–11545. [[CrossRef](#)]
94. Nakamura, K.; Fujimoto, T.; Takara, S.; Sugiura, K.-I.; Miyasaka, H.; Ishii, T.; Yamashita, M.; Sakata, Y. Systematic synthesis of porphyrin dimers linked by conjugated oligoacetylene bridges. *Chem. Lett.* **2003**, *32*, 694–695. [[CrossRef](#)]
95. Hayashi, N.; Sato, M.; Miyabayashi, K.; Miyake, M.; Higuchi, H. Synthesis and electronic properties of trimeric octaethylporphyrin (OEP) derivative connected with diacetylene linkage. A comparative study with vinylene-group connected OEP trimer. *Sci. Technol. Adv. Mater.* **2006**, *7*, 237–242. [[CrossRef](#)]
96. Yamada, H.; Kushibe, K.; Mitsuogi, S.; Okujima, T.; Uno, H.; Ono, N. Selective synthesis of 5-alkenyl-15-alkynyl-porphyrin and 5,15-dialkynyl-porphyrin by 2+2 acid-catalyzed condensation of dipyrromethane and TMS propynal. *Tetrahedron Lett.* **2008**, *49*, 4731–4733. [[CrossRef](#)]
97. Hiroyuki, H.; Takashi, I.; Kazumine, M.; Yukari, T.; Koji, Y.; Keita, T.; Keiko, M.; Mikio, M. Synthesis and Properties of Head-to-head, Head-to-tail, and Tail-to-tail Orientational Isomers of Extended Dihexylbithiophene–Octaethylporphyrin System [OEP–(DHBT) $n$ –OEP] Connected with 1,3-Butadiyne Linkages. *Bull. Chem. Soc. Jpn.* **2001**, *74*, 889–906. [[CrossRef](#)]
98. Kanwal, I.; Mujahid, A.; Rasool, N.; Rizwan, K.; Malik, A.; Ahmad, G.; Shah, S.A.A.; Rashid, U.; Nasir, N.M. Palladium and Copper Catalyzed Sonogashira cross Coupling an Excellent Methodology for C–C Bond Formation over 17 Years: A Review. *Catalysts* **2020**, *10*, 443. [[CrossRef](#)]
99. Gou, F.; Jiang, X.; Fang, R.; Jing, H.; Zhu, Z. Strategy to Improve Photovoltaic Performance of DSSC Sensitized by Zinc Porphyrin Using Salicylic Acid as a Tridentate Anchoring Group. *ACS Appl. Mater. Interfaces* **2014**, *6*, 6697–6703. [[CrossRef](#)]
100. Chen, Y.-J.; Lee, G.-H.; Peng, S.-M.; Yeh, C.-Y. Unexpected formation of porphyrinic enyne under Sonogashira conditions. *Tetrahedron Lett.* **2005**, *46*, 1541–1544. [[CrossRef](#)]
101. Chang, J.-C.; Ma, C.-J.; Lee, G.-H.; Peng, S.-M.; Yeh, C.-Y. Porphyrin–triarylamine conjugates: Strong electronic communication between triarylamine redox centers via the porphyrin dication. *Dalton Trans.* **2005**, 1504–1508. [[CrossRef](#)]
102. Dy, J.T.; Maeda, R.; Nagatsuka, Y.; Ogawa, K.; Kamada, K.; Ohta, K.; Kobuke, Y. A photochromic porphyrin–perinaphthothioindigo conjugate and its two-photon absorption properties. *Chem. Commun.* **2007**, 1504–1508. [[CrossRef](#)]
103. Wada, T.; Tachi, Y.; Toyota, K.; Kozaki, M. Platinum octaethylporphyrin-diphenylanthracene dyad with an ethynylene linker. *Tetrahedron Lett.* **2022**, *108*, 154131. [[CrossRef](#)]
104. Zhang, T.-G.; Zhao, Y.; Asselberghs, I.; Persoons, A.; Clays, K.; Therien, M.J. Design, Synthesis, Linear, and Nonlinear Optical Properties of Conjugated (Porphinato)zinc(II)-Based Donor–Acceptor Chromophores Featuring Nitrothiophenyl and Nitrooligothiophenyl Electron-Accepting Moieties. *J. Am. Chem. Soc.* **2005**, *127*, 9710–9720. [[CrossRef](#)]
105. Zhang, T.-G.; Zhao, Y.; Song, K.; Asselberghs, I.; Persoons, A.; Clays, K.; Therien, M.J. Electronic Modulation of Hyperpolarizable (Porphinato)zinc(II) Chromophores Featuring Ethynylphenyl-, Ethynylthiophenyl-, Ethynylthiazolyl-, and Ethynylbenzothiazolyl-Based Electron-Donating and -Accepting Moieties. *Inorg. Chem.* **2006**, *45*, 9703–9712. [[CrossRef](#)] [[PubMed](#)]



106. Bessho, T.; Zakeeruddin, S.M.; Yeh, C.-Y.; Diau, E.W.-G.; Grätzel, M. Highly Efficient Mesoscopic Dye-Sensitized Solar Cells Based on Donor–Acceptor-Substituted Porphyrins. *Angew. Chem. Int. Ed.* **2010**, *49*, 6646–6649. [[CrossRef](#)] [[PubMed](#)]
107. Lee, C.-W.; Lu, H.-P.; Lan, C.-M.; Huang, Y.-L.; Liang, Y.-R.; Yen, W.-N.; Liu, Y.-C.; Lin, Y.-S.; Diau, E.W.-G.; Yeh, C.-Y. Novel Zinc Porphyrin Sensitizers for Dye-Sensitized Solar Cells: Synthesis and Spectral, Electrochemical, and Photovoltaic Properties. *Chem.—A Eur. J.* **2009**, *15*, 1403–1412. [[CrossRef](#)]
108. Marschner, S.M.; Haldar, R.; Fuhr, O.; Wöll, C.; Bräse, S. Modular Synthesis of trans-A2B2-Porphyrins with Terminal Esters: Systematically Extending the Scope of Linear Linkers for Porphyrin-Based MOFs. *Chem.—A Eur. J.* **2021**, *27*, 1390–1401. [[CrossRef](#)]
109. Felix, L.; Sezer, U.; Arndt, M.; Mayor, M. Synthesis of Highly Fluoroalkyl-Functionalized Oligoporphyrin Systems. *Eur. J. Org. Chem.* **2014**, *2014*, 6884–6895. [[CrossRef](#)]
110. Wagner, R.W.; Johnson, T.E.; Lindsey, J.S. Soluble Synthetic Multiporphyrin Arrays. 1. Modular Design and Synthesis. *J. Am. Chem. Soc.* **1996**, *118*, 11166–11180. [[CrossRef](#)]
111. Wagner, R.W.; Johnson, T.E.; Li, F.; Lindsey, J.S. Synthesis of Ethyne-Linked or Butadiyne-Linked Porphyrin Arrays Using Mild, Copper-Free, Pd-Mediated Coupling Reactions. *J. Org. Chem.* **1995**, *60*, 5266–5273. [[CrossRef](#)]
112. Yamamoto, T.; Kato, K.; Shimizu, D.; Tanaka, T.; Osuka, A. Phenylene-bridged Porphyrin meso-Oxy Radical Dimers. *Chem.—Asian J.* **2019**, *14*, 4031–4034. [[CrossRef](#)]
113. Okuno, Y.; Kamikado, T.; Yokoyama, S.; Mashiko, S. Determining the conformation of a phenylene-linked porphyrin dimer by NMR spectroscopy and quantum chemical calculations. *J. Mol. Struct. THEOCHEM* **2003**, *631*, 13–20. [[CrossRef](#)]
114. Taylor, P.N.; Wylie, A.P.; Huuskonen, J.; Anderson, H.L. Enhanced Electronic Conjugation in Anthracene-Linked Porphyrins. *Angew. Chem. Int. Ed.* **1998**, *37*, 986–989. [[CrossRef](#)]
115. Drobizhev, M.; Stepanenko, Y.; Dzenis, Y.; Karotki, A.; Rebane, A.; Taylor, P.N.; Anderson, H.L. Understanding Strong Two-Photon Absorption in  $\pi$ -Conjugated Porphyrin Dimers via Double-Resonance Enhancement in a Three-Level Model. *J. Am. Chem. Soc.* **2004**, *126*, 15352–15353. [[CrossRef](#)] [[PubMed](#)]
116. Balaz, M.; Collins, H.A.; Dahlstedt, E.; Anderson, H.L. Synthesis of hydrophilic conjugated porphyrin dimers for one-photon and two-photon photodynamic therapy at NIR wavelengths. *Org. Biomol. Chem.* **2009**, *7*, 874–888. [[CrossRef](#)] [[PubMed](#)]
117. Sugiura, K.-I.; Fujimoto, Y.; Sakata, Y. A porphyrin square: Synthesis of a square-shaped  $\pi$ -conjugated porphyrin tetramer connected by diacetylene linkages. *Chem. Commun.* **2000**, 1105–1106. [[CrossRef](#)]
118. Taylor, P.N.; Huuskonen, J.; Aplin, R.T.; Anderson, H.L.; Huuskonen, J.; Rumbles, G.; Williams, E. Conjugated porphyrin oligomers from monomer to hexamer. *Chem. Commun.* **1998**, 909–910. [[CrossRef](#)]
119. Aiko, K.; Ken-ichi, S.; Hitoshi, M.; Hiroyuki, T.; Tomoji, K.; Manabu, S.; Masahiro, Y. A Square Cyclic Porphyrin Dodecamer: Synthesis and Single-Molecule Characterization. *Chem. Lett.* **2004**, *33*, 578–579. [[CrossRef](#)]
120. Hoffmann, M.; Wilson, C.J.; Odell, B.; Anderson, H.L. Template-Directed Synthesis of a  $\pi$ -Conjugated Porphyrin Nanoring. *Angew. Chem. Int. Ed.* **2007**, *46*, 3122. [[CrossRef](#)]
121. Hoffmann, M.; Kärnbratt, J.; Chang, M.-H.; Herz, L.M.; Albinsson, B.; Anderson, H.L. Enhanced  $\pi$  Conjugation around a Porphyrin[6] Nanoring. *Angew. Chem. Int. Ed.* **2008**, *47*, 4993–4996. [[CrossRef](#)]
122. Nakamura, Y.; Aratani, N.; Osuka, A. Cyclic porphyrin arrays as artificial photosynthetic antenna: Synthesis and excitation energy transfer. *Chem. Soc. Rev.* **2007**, *36*, 831–845. [[CrossRef](#)]
123. Wang, S.-P.; Shen, Y.-F.; Zhu, B.-Y.; Wu, J.; Li, S. Recent advances in the template-directed synthesis of porphyrin nanorings. *Chem. Commun.* **2016**, *52*, 10205–10216. [[CrossRef](#)]
124. Ryan, A.; Gehrold, A.; Perusitti, R.; Pinteá, M.; Fazekas, M.; Locos, O.B.; Blaikie, F.; Senge, M.O. Porphyrin Dimers and Arrays. *Eur. J. Org. Chem.* **2011**, *2011*, 5817–5844. [[CrossRef](#)]
125. Zawadzka, M.; Wang, J.; Blau, W.J.; Senge, M.O. Correlation studies on structurally diverse porphyrin monomers, dimers and trimers and their nonlinear optical responses. *Chem. Phys. Lett.* **2009**, *477*, 330–335. [[CrossRef](#)]
126. Maeda, C.; Yamaguchi, S.; Ikeda, C.; Shinokubo, H.; Osuka, A. Dimeric Assemblies from 1,2,3-Triazole-Appended Zn(II) Porphyrins with Control of NH-Tautomerism in 1,2,3-Triazole. *Org. Lett.* **2008**, *10*, 549–552. [[CrossRef](#)]
127. Séverac, M.; Pleux, L.L.; Scarpaci, A.; Blart, E.; Odobel, F. Synthesis of new azido porphyrins and their reactivity in copper(I)-catalyzed Huisgen 1,3-dipolar cycloaddition reaction with alkynes. *Tetrahedron Lett.* **2007**, *48*, 6518–6522. [[CrossRef](#)]
128. Shen, D.-M.; Liu, C.; Chen, Q.-Y. Synthesis and Versatile Reactions of  $\beta$ -Azidotetraarylporphyrins. *Eur. J. Org. Chem.* **2007**, *2007*, 1419–1422. [[CrossRef](#)]
129. Thorley, K.J.; Anderson, H.L. Extending conjugation in porphyrin dimer carbocations. *Org. Biomol. Chem.* **2010**, *8*, 3472–3479. [[CrossRef](#)]

**Disclaimer/Publisher’s Note:** The statements, opinions and data contained in all publications are solely those of the individual author(s) and contributor(s) and not of MDPI and/or the editor(s). MDPI and/or the editor(s) disclaim responsibility for any injury to people or property resulting from any ideas, methods, instructions or products referred to in the content.